INTERNATIONAL JOURNAL OF
NUMERICAL ANALYSIS AND MODELING
Volume 22, Number 4, Pages 510–533

doi: 10.4208/ijnam2025-1022

AN UNCONDITIONALLY ENERGY-STABLE SAV-DG NUMERICAL SCHEME FOR TUMOR GROWTH MODEL

PENGHAO GUO, BO WANG*, AND GUANG-AN ZOU

Abstract. In this paper, we propose a linear, fully decoupled and unconditionally energy-stable discontinuous Galerkin (DG) method for solving the tumor growth model, which is derived from the variation of the free energy. The fully discrete scheme is constructed by the scalar auxiliary variable (SAV) for handling the nonlinear term and backward Euler method for the time discretization. We rigorously prove the unconditional energy stability and optimal error estimates of the scheme. Finally, several numerical experiments are performed to verify the energy stability and validity of the proposed scheme.

Key words. Tumor growth model, DG method, SAV approach, optimal error estimates.

1. Introduction

According to the International Agency for Research on Cancer (IARC), the malignant tumor has become one of the major diseases affecting human health in the world [1–4]. Due to the lack of understanding the mechanisms of tumor growth, many difficulties have been encountered in the treatment process [5, 6]. The research of tumor growth holds significance for clinical therapy, thereby generating considerable interest from the fields of medicine, genetics and biology [7–11]. As we know, an accurate mathematical model will help medical staff to better understand the mechanism of tumor growth [12–15].

Recently, many researchers have focused on the mathematical models for investigating the tumor growth [16–22]. In order to better predict the evolution of tumor, the phase-field model has been widely used to study the tumor growth [23–28]. In [23] the authors used the Cahn-Hilliard equation to describe multispecies tumor growth and tumor-induced angiogenesis. In [24], the Cahn-Hilliard type equation with degenerate mobility had been used to simulate the evolution and growth of solid tumors. In [27] the authors introduced the Allen-Cahn equation to describe the progression of tumoral expansion within the growth region. In this study, we derive the tumor growth model based on the law of energy conservation in the polygonal domain Ω in $\mathbb{R}^d$ $(d = 2, 3)$. The total free energy of the system is defined as

$$E(\phi,\sigma) = \int_\Omega [F(\phi) + \frac{\lambda}{2}|\nabla\phi|^2 + \frac{\alpha}{2}\phi^2 + \frac{\beta}{2}|\nabla\sigma|^2 - (\chi\phi - \frac{\gamma}{2}\sigma + s)\sigma]\, d\boldsymbol{x}, \tag{1}$$

with the following double-well type potential

$$F(\phi) = \frac{16}{\varepsilon}\phi^2(1-\phi)^2,$$

where $\varepsilon > 0$ is the time scale. By using gradient flow method [29–31], the following equation can be derived as

$$\phi_t = -\frac{\delta E}{\delta\phi} = \lambda\Delta\phi - f(\phi) + \chi\sigma - \alpha\phi, \qquad \text{in } \Omega\times(0,T), \tag{2a}$$

Received by the editors on February 24, 2024 and, accepted on September 26, 2024.
2000 *Mathematics Subject Classification.* 35Q35, 65M12, 65M15, 65M60.
*Corresponding author.

$$\sigma_t = -\frac{\delta E}{\delta \sigma} = \beta \Delta \sigma + s + \chi \phi - \gamma \sigma, \qquad \text{in } \Omega \times (0, T), \tag{2b}$$

subject with the following initial and the boundary conditions

$$\phi(\boldsymbol{x}, 0) = \phi_0, \ \sigma(\boldsymbol{x}, 0) = \sigma_0, \qquad \text{in } \Omega, \tag{3a}$$

$$\partial_{\boldsymbol{n}} \phi(\boldsymbol{x}, t) = 0, \ \partial_{\boldsymbol{n}} \sigma(\boldsymbol{x}, t) = 0, \qquad \text{on } \partial\Omega, \tag{3b}$$

where $f(\phi) = F'(\phi)$ and $\boldsymbol{n}$ is the unit outward normal vector on $\partial\Omega$. The unknown functions ϕ and σ are the phase function and the concentration of the nutrient, respectively. The physical parameters λ represents the phase field diffusion coefficient, χ denotes the rate of tumor growth, α is the rate of normal cell apoptosis, β represents the nutrient diffusion coefficient, s denotes the sustained supply of the nutrient, and γ is the natural decay of the nutrient, which are positive.

To the best of the author's knowledge, most of the researches related to tumor growth model have focused on numerical simulations and numerical analysis [23–28, 32–38]. Lorenzo et al. [33] used isometric analysis to solve the Allen-Cahn equation and simulated the tumor growth process. In what follows, Mohammadi et al. [34,35] also simulated the same model numerically by applying the finite difference method and the meshless method. For describing the growth dynamics of avascular tumors, Medina et al. developed a hybrid discontinuous Galerkin numerical scheme for the Cahn-Hilliard equation in [36]. However, the above-mentioned researches lack the stability and optimal error estimates of the coupled model. Agosti et al. [24] employed the finite element method to discrete the Cahn-Hilliard equation, and proved the existence and uniqueness of the proposed semi-discrete scheme, without the convergence analysis. In [37], Xu et al. used the BDF1 method to construct a linear, fully decoupled and energy stable numerical scheme for the Cahn-Hilliard-Navier-Stokes system, and derived the optimal error estimates. However, it should be noted that the proposed scheme is semi-discrete in time. For the Cahn-Hilliard-Brinkman-Ohta-Kawaski tumor growth model, the authors in [38] proposed a fully discrete numerical scheme with the H^1-norm optimal error estimates by using the discontinuous Galerkin (DG) method. They verified the validity and stability of the proposed scheme through several numerical experiments.

Note that constructing an efficient numerical scheme for the tumor growth model is definitely not a simple task due to highly nonlinear term and strongly coupled term. First of all, the main difficulty caused by the nonlinear term in model (2) is how to propose an effective energy stable time discrete strategy for solving the corresponding phase field equation. We use the scalar auxiliary variable (SAV) method [39–44] to deal with the nonlinear term and transform the original equation into an equivalent linear system. Furthermore, the diffusion term in the phase field equation produces a discontinuity at the phase transition boundary, and the discontinuous Galerkin (DG) method [45–54] performs well for the complex boundary problems. In this paper, we develop a fully discrete DG scheme which is linear, full decoupled and unconditionally energy stable. In addition, the unique solvability and the L^2-norm optimal error estimates are given in details. Finally, the stability and validity of the proposed scheme is verified by a series of numerical experiments.

The outline of this paper is organized as follows. Section 2 demonstrates that the tumor growth model is unconditionally energy dissipative. In Section 3, we develop a linear, decoupled fully discrete numerical scheme, and derive the unique solvability and discrete energy law. The prove of optimal error estimates for the fully discrete scheme is given in Section 4. In Section 5, we present some numerical

experiments to illustrate the theoretical analysis. The last Section draws some concluding remarks.

2. Preliminaries

For $1 \leq p \leq \infty$, and $k \geq 0$, we use $W^{k,p}(\Omega)$ to denote the standard Sobolev spaces with the order k will also be used, which equipped with the norm $\|\cdot\|_{W^{k,p}}$. Particularly, we denote the Hilbert space $H^k(\Omega) = W^{k,2}(\Omega)$ with norm $\|\cdot\|_{H^k}$. We denote the Lebesgue spaces $L^p(\Omega) = W^{0,p}(\Omega)$ equipped with the norm $\|\cdot\|_{L^p} := (\int_\Omega |\cdot|^p d\boldsymbol{x})^{\frac{1}{p}}$, and $L^p([0,T])$ equipped with the norm $\|\cdot\|_{L^p} := (\int_0^T |\cdot|^p dt)^{\frac{1}{p}}$. Both of them use the abbreviation L^p, we also denote by $\|\cdot\|$ and $(\cdot,\cdot)$ the norm and inner product of $L^2(\Omega)$.

The function space is defined as follows

$$M := H_0^1(\Omega) := \{\varphi \in H^1(\Omega) : \varphi = 0 \text{ on } \partial\Omega\}.$$

Lemma 2.1. *The system (2) poessess the following energy law*

$$\frac{d}{dt}E(\phi,\sigma) + \|\phi_t\|^2 + \|\sigma_t\|^2 = 0. \tag{4}$$

Proof. By taking the L^2 inner product of (2a) with ϕ_t, and (2b) with σ_t performing integration by parts, and adding these relations we easily derive the energy law (4). □

We adopt a novel approach called SAV to address the nonlinear potential in (2). Firstly, an energy function is introduced by

$$E_1(\phi) = \int_\Omega F(\phi) d\boldsymbol{x} + B, \tag{5}$$

in which B is a positive constant ensuring that $E_1(\phi) > 0$ is established. Then, the original energy $E(\phi,\sigma)$ can be written as

(6)
$$\begin{aligned} E_{tot}(\phi,\sigma) &= \int_\Omega [\frac{\lambda}{2}|\nabla\phi|^2 + \frac{\alpha}{2}\phi^2 + \frac{\beta}{2}|\nabla\sigma|^2 - (\chi\phi - \frac{\gamma}{2}\sigma + s)\sigma] d\boldsymbol{x} + E_1(\phi) - B \\ &= \int_\Omega [\frac{\lambda}{2}|\nabla\phi|^2 + \frac{\alpha}{2}\phi^2 + \frac{\beta}{2}|\nabla\sigma|^2 - (\chi\phi - \frac{\gamma}{2}\sigma + s)\sigma] d\boldsymbol{x} + |R(t)|^2 - B, \end{aligned}$$

where the auxiliary variable is defined as

$$R(t) = \sqrt{E_1(\phi)}. \tag{7}$$

We can rewrite (2) into the following equivalent system

$$\phi_t = \lambda\Delta\phi - \frac{R(t)}{\sqrt{E_1(\phi)}} f(\phi) + \chi\sigma - \alpha\phi, \tag{8a}$$

$$\sigma_t = \beta\Delta\sigma + s + \chi\phi - \gamma\sigma, \tag{8b}$$

$$R_t = \int_\Omega \frac{f(\phi)}{2\sqrt{E_1(\phi)}} \phi_t \, d\boldsymbol{x}. \tag{8c}$$

Here we have $R(0) = \sqrt{E_1(\phi_0)}$ for any $\boldsymbol{x} \in \Omega$ as the initial condition of the equation (8c).

The weak form based on the SAV scheme is: Find $(\phi, \sigma, R) \in M \times M \times \mathbb{R}$ for all $(\theta, \omega) \in M \times M$, there holds

$$(\phi_t, \theta) = -\lambda(\nabla\phi, \nabla\theta) - \frac{R(t)}{\sqrt{E_1(\phi)}}(f(\phi), \theta) + \chi(\sigma, \theta) - \alpha(\phi, \theta), \tag{9a}$$

$$(\sigma_t, \omega) = -\beta(\nabla\sigma, \nabla\omega) + (s, \omega) + \chi(\phi, \omega) - \gamma(\sigma, \omega), \tag{9b}$$

$$R_t = \int_\Omega \frac{f(\phi)}{2\sqrt{E_1(\phi)}}\phi_t \, d\boldsymbol{x}. \tag{9c}$$

Lemma 2.2. *The same energy dissipation law is complied by the system* (9)

$$\frac{d}{dt}E_{tot}(\phi, \sigma) + \|\phi_t\|^2 + \|\sigma_t\|^2 = 0. \tag{10}$$

Proof. By choosing $\theta = \phi_t$ in (9a), and $\omega = \sigma_t$ in (9b), then multiplying (9c) by $2R(t)$, adding these results together yields

$$\begin{aligned}&(\phi_t, \phi_t) + \lambda(\nabla\phi, \nabla\phi_t) - \chi(\sigma, \phi_t) + \alpha(\phi, \phi_t) + \beta(\nabla\sigma, \nabla\sigma_t)\\ &+ (\sigma_t, \sigma_t) - (s, \sigma_t) - \chi(\phi, \sigma_t) + \gamma(\sigma, \sigma_t) + 2RR_t = 0,\end{aligned}$$

then, one can obtian

$$\begin{aligned}&\frac{\lambda}{2}\frac{d}{dt}\|\nabla\phi\|^2 + \frac{\beta}{2}\frac{d}{dt}\|\nabla\sigma\|^2 + \frac{\alpha}{2}\frac{d}{dt}\|\phi\|^2 + \frac{\gamma}{2}\frac{d}{dt}\|\sigma\|^2\\ &- \chi\frac{d}{dt}(\phi, \sigma) - \frac{d}{dt}(s, \sigma) + \frac{d}{dt}|R|^2 + \|\phi_t\|^2 + \|\sigma_t\|^2 = 0.\end{aligned}$$

After a simple treatment, the intended result (10) is achieved. □

3. The SAV-DG scheme

Let $\mathcal{E}_h$ denote the regular triangulation of Ω, with $E \in \mathcal{E}_h$ denoting a mesh element of the subdivision. Let $h_E = diam(E)$ and $h = \max\limits_{E\in\mathcal{E}_h} h_E$. In subdivision $\mathcal{E}_h$, we use Γ_h to denote the set of interior edges. We write $|e|$ for its length for $\forall e \in \Gamma_h$ shared by elements E_e^1 and E_e^2. Let $\boldsymbol{n}_e$ represent the unit normal vector oriented from E_e^1 to E_e^2, where E_e^1 and E_e^2 are the two elements adjacent to e. Let $\boldsymbol{n}_e$ is the unit outward normal vector to $\partial\Omega$, when e is on the boundary $\partial\Omega$. We define average and jump operators for v as follows

$$\begin{aligned}&\forall e \in \partial E_e^1 \cap \partial E_e^2, && [v] = v|_{E_e^1} - v|_{E_e^2}, && \{v\} = \frac{1}{2}(v|_{E_e^1} + v|_{E_e^2}),\\ &\forall e \in \partial E_e^1 \cap \partial\Omega, && [v] = v|_{E_e^1}, && \{v\} = v|_{E_e^1}.\end{aligned}$$

We then denote the broken polynomial spaces for ϕ and σ as follows

$$M_h = \{\varphi_h \in L^2(\Omega) : \forall E \in \mathcal{E}_h,\ \varphi_h|_E \in \mathbb{P}_k(E)\}.$$

For any fixed positive integer $k \geq 1$, $\mathbb{P}_k(E)$ is the space consisting of polynomials with degree at most k defined on E.

Based on the above discrete Sobolev spaces, we introduce the following energy norms

$$\begin{aligned}&\forall\theta \in M_h, \quad \|\theta\|_{DG} := \Big(\sum_{E\in\mathcal{E}_h}\|\nabla\theta\|^2_{L^2(E)} + \sum_{e\in\Gamma_h\cup\partial\Omega}\frac{\sigma_e}{|e|}\|[\theta]\|^2_{L^2(e)}\Big)^{\frac{1}{2}},\\ &\forall\omega \in M_h, \quad \|\omega\|_{DG} := \Big(\sum_{E\in\mathcal{E}_h}\|\nabla\omega\|^2_{L^2(E)} + \sum_{e\in\Gamma_h\cup\partial\Omega}\frac{\sigma_e}{|e|}\|[\omega]\|^2_{L^2(e)}\Big)^{\frac{1}{2}}.\end{aligned}$$

For convenience, we denote the generic constant by C, which is independent of the time step Δt and the mesh size h. Whenever no confusion, we write $a \leq Cb$ as $a \lesssim b$ for brevity.

Now we will give the detailed definitions of bilinear forms. The forms $\mathcal{A}_1$ and $\mathcal{A}_2$ are defined respectively by

$$\begin{aligned}\forall \phi, \theta \in M_h, \quad \mathcal{A}_1(\phi,\theta) = &\sum_{E\in\mathcal{E}_h} (\nabla\phi, \nabla\theta)_E - \sum_{e\in\Gamma_h\cup\partial\Omega} (\{\nabla\phi\cdot\boldsymbol{n}_e\}, [\theta])_e \\ &- \sum_{e\in\Gamma_h\cup\partial\Omega} (\{\nabla\theta\cdot\boldsymbol{n}_e\}, [\phi])_e + \sum_{e\in\Gamma_h\cup\partial\Omega} \frac{\sigma_e}{|e|}([\phi],[\theta])_e, \\ \forall \sigma, \omega \in M_h, \quad \mathcal{A}_2(\sigma,\omega) = &\sum_{E\in\mathcal{E}_h} (\nabla\sigma, \nabla\omega)_E - \sum_{e\in\Gamma_h\cup\partial\Omega} (\{\nabla\sigma\cdot\boldsymbol{n}_e\}, [\omega])_e \\ &- \sum_{e\in\Gamma_h\cup\partial\Omega} (\{\nabla\omega\cdot\boldsymbol{n}_e\}, [\sigma])_e + \sum_{e\in\Gamma_h\cup\partial\Omega} \frac{\sigma_e}{|e|}([\sigma],[\omega])_e,\end{aligned}$$

where $\sigma_e > 0$ is the penalty parameter should be chosen large enough.

The following operators, which are essential in numerical schemes and error analysis, will be introduced. We use the broken elliptic projection operators $\mathcal{Q}_h : H^1(\Omega) \to M_h$ and $\mathcal{F}_h : H^1(\Omega) \to M_h$ throughout this paper (see [48]), which are defined as

$$\forall \phi \in H^1(\Omega),\ \forall \theta \in M_h, \qquad \mathcal{A}_1(\phi - \mathcal{Q}_h\phi, \theta) = 0, \tag{11}$$

$$\forall \sigma \in H^1(\Omega),\ \forall \omega \in M_h, \qquad \mathcal{A}_2(\sigma - \mathcal{F}_h\sigma, \omega) = 0. \tag{12}$$

And then, the following estimates will be obtained (see [48])

$$\begin{aligned}&\|\phi(t) - \mathcal{Q}_h\phi(t)\|_{DG} \lesssim h^k \|\phi(t)\|_{H^{k+1}(\Omega)}, \\ &\|\phi(t) - \mathcal{Q}_h\phi(t)\|_{L^2(\Omega)} \lesssim h^{k+1} \|\phi(t)\|_{H^{k+1}(\Omega)}, \\ &\|\sigma(t) - \mathcal{F}_h\sigma(t)\|_{DG} \lesssim h^k \|\sigma(t)\|_{H^{k+1}(\Omega)}, \\ &\|\sigma(t) - \mathcal{F}_h\sigma(t)\|_{L^2(\Omega)} \lesssim h^{k+1} \|\sigma(t)\|_{H^{k+1}(\Omega)}.\end{aligned} \tag{13}$$

3.1. Numerical scheme. Let $t_n = n\Delta t$ be a uniform partition of the time interval $[0, T]$, $0 \leq n \leq N$, with $\Delta t = T/N$. For simplicity, we give the following denotation

$$\delta_t v_h^{n+1} = \frac{v_h^{n+1} - v_h^n}{\Delta t},\ \delta_t v(t_{n+1}) = \frac{v(t_{n+1}) - v(t_n)}{\Delta t}.$$

Next, we present the fully discrete DG scheme of system (9).

Step 1: Find $(\phi_h^{n+1}, R_h^{n+1}) \in (M_h, \mathbb{R})$ such that for all $\theta_h \in M_h$, there holds

$$\begin{aligned}(\frac{\phi_h^{n+1} - \phi_h^n}{\Delta t}, \theta_h) = &-\lambda\mathcal{A}_1(\phi_h^{n+1}, \theta_h) - \frac{R_h^{n+1}}{\sqrt{E_1(\phi_h^n)}}(f(\phi_h^n), \theta_h) \\ &+ \chi(\sigma_h^n, \theta_h) - \alpha(\phi_h^{n+1}, \theta_h),\end{aligned} \tag{14a}$$

$$R_h^{n+1} - R_h^n = \frac{1}{2\sqrt{E_1(\phi_h^n)}}(f(\phi_h^n), \phi_h^{n+1} - \phi_h^n), \tag{14b}$$

where $E_1(\phi_h^n)$ and R_h^{n+1} in (14a)-(14b) are given by

$$\begin{cases} E_1(\phi_h^n) = \int_\Omega F(\phi_h^n) d\boldsymbol{x} + B, \\ R_h^{n+1} = \sqrt{E_1(\phi_h^{n+1})}. \end{cases}$$

Step 2: Find $\sigma_h^{n+1} \in M_h$ such that for all $\omega_h \in M_h$, there holds

$$(\frac{\sigma_h^{n+1}-\sigma_h^n}{\Delta t},\omega_h) = -\beta\mathcal{A}_2(\sigma_h^{n+1},\omega_h) + \chi(\phi_h^{n+1},\omega_h) + (s,\omega_h) - \gamma(\sigma_h^{n+1},\omega_h), \tag{15}$$

with the following initial conditions

$$\phi_h^0 = \mathcal{Q}_h\phi^0, \sigma_h^0 = \mathcal{F}_h\sigma^0, R_h^0 = \sqrt{E_1(\phi_h^0)}. \tag{16}$$

3.2. Well-posedness. We first introduce several important results frequently used in this paper, and then show the well-posedness of the considered scheme.

Lemma 3.1. *(see [48]) The bilinear forms $\mathcal{A}_1$ and $\mathcal{A}_2$ satisfy the following properties*

$$\begin{aligned} &\forall \phi,\theta \in M_h, \quad \mathcal{A}_1(\theta,\theta) \gtrsim \|\theta\|_{DG}^2, \quad \mathcal{A}_1(\phi,\theta) \lesssim \|\phi\|_{DG}\|\theta\|_{DG}, \\ &\forall \sigma,\omega \in M_h, \quad \mathcal{A}_2(\omega,\omega) \gtrsim \|\theta\|_{DG}^2, \quad \mathcal{A}_2(\sigma,\omega) \lesssim \|\sigma\|_{DG}\|\omega\|_{DG}. \end{aligned} \tag{17}$$

From the coercivity of $\mathcal{A}_1$ and $\mathcal{A}_2$, one can easily get that $\mathcal{A}_1(\theta,\theta) \geq 0$ and $\mathcal{A}_2(\omega,\omega) \geq 0$. In addition, broken DG (semi) norm $|||\cdot|||$ is defined by

$$|||\theta|||^2 = \mathcal{A}_1(\theta,\theta), \ |||\omega|||^2 = \mathcal{A}_2(\omega,\omega). \tag{18}$$

Lemma 3.2. *(Broken Sobolev Poincaré inequality, see [48]) There exist some contants independent of h, such that*

$$\|\theta\|_{L^p(\Omega)} \lesssim \|\theta\|_{DG}, \tag{19}$$

for all $\theta \in M_h$, $2 \leq p < \infty$ when $d = 2$ and $2 \leq p \leq 6$ when $d = 3$.

Lemma 3.3. *(Discrete Gronwalls lemma, see [48]) Let $\{a_n\}$, $\{b_n\}$ and $\{c_n\}$ be nonnegative real sequences, for constants $\Delta t > 0$, $B > 0$ and $C > 0$*

$$\begin{aligned} &if\ a_m + \Delta t\sum_{i=0}^{m} b_i \leq C\Delta t\sum_{i=0}^{m} a_i + \Delta t\sum_{i=0}^{m} c_i + B,\ C\Delta t < 1, \\ &then\ a_m + \Delta t\sum_{i=0}^{m} b_i \leq e^{C(n+1)\Delta t}(B + \Delta t\sum_{i=0}^{m} c_i),\ \forall m \geq 0. \end{aligned} \tag{20}$$

Lemma 3.4. *(Trace inequality, see [48]) For a bounded domain E in $\mathbb{R}^2$, such that*

$$\begin{aligned} &\forall \theta \in \mathbb{P}_k(E), e \in \partial E, \quad \|\theta\|_{L^2(e)} \lesssim h_E^{-1/2}\|\theta\|_{L^2(E)}, \\ &\forall \theta \in \mathbb{P}_k(E), e \in \partial E, \quad \|\nabla\theta\cdot\boldsymbol{n}\|_{L^2(e)} \lesssim h_E^{-1/2}\|\nabla\theta\|_{L^2(E)}, \end{aligned} \tag{21}$$

where h_E and e are diameter and side of E, respectively.

To focus on the well-posedness of the given scheme, we demonstrate the existence and uniqueness of numerical solution using the Lax-Milgram theorem.

Theorem 3.5. *(Unique solvability) The scheme (14)-(15) admits a unique solution $(\phi_h^{n+1}, \sigma_h^{n+1}, R_h^{n+1}) \in (M_h, M_h, \mathbb{R})$.*

Proof. To begin with, we define a bilinear form $\mathcal{F}(\cdot,\cdot) : (M_h, M_h, \mathbb{R})\times(M_h, M_h, \mathbb{R}) \to \mathbb{R}$ by

(22)

$$\begin{aligned} \mathcal{F}((\phi,\sigma,R),(\theta,\omega,Q)) = {} & (\phi,\theta) + \lambda\Delta t\mathcal{A}_1(\phi,\theta) + \alpha\Delta t(\phi,\theta) + \Delta t\frac{R}{\sqrt{E_1(\phi_h^n)}}(f(\phi_h^n),\theta) \\ & + 2\Delta tRQ + (\sigma,\omega) - \Delta t\frac{Q}{\sqrt{E_1(\phi_h^n)}}(f(\phi_h^n),\phi) \\ & + \beta\Delta t\mathcal{A}_2(\sigma,\omega) - \chi\Delta t(\phi,\omega) + \gamma\Delta t(\sigma,\omega), \end{aligned}$$

and a linear form by $L(\cdot):(M_h,M_h,\mathbb{R})\to\mathbb{R}$, namely

$$\begin{aligned}L(\theta,\omega,Q)=&(\phi_h^n,\theta)+\chi\Delta t(\sigma_h^n,\theta)+2\Delta tR_h^nQ+(\sigma_h^n,\omega)\\&-\Delta t\frac{Q}{\sqrt{E_1(\phi_h^n)}}(f(\phi_h^n),\phi_h^n)+\Delta t(s,\omega).\end{aligned}\tag{23}$$

Then, (14)-(15) can be expressed as: find $(\phi_h^{n+1},\sigma_h^{n+1},R_h^{n+1})\in(M_h,M_h,\mathbb{R})$ such that for any $(\theta_h,\omega_h,Q_h)\in(M_h,M_h,\mathbb{R})$, there holds

$$\mathcal{F}((\phi_h^{n+1},\omega_h^{n+1},\mathbb{R}_h^{n+1}),(\theta_h,\omega_h,Q_h))=L(\theta_h,\omega_h,Q_h).\tag{24}$$

Using the Cauchy-Schwarz inequality and Lemma 3.1, we can infer that $\mathcal{F}(\cdot,\cdot)$ is bounded, namely

$$\begin{aligned}&\mathcal{F}((\phi,\sigma,R),(\theta,\omega,Q))\\&\le\|\phi\|\|\theta\|+\lambda\Delta t\|\phi\|_{DG}\|\theta\|_{DG}+\alpha\Delta t\|\phi\|\|\theta\|+\Delta t|R|\|\theta\|+2\Delta t|R||Q|\\&\quad+\Delta t|Q|\|\phi\|+\|\sigma\|\|\omega\|+\beta\Delta t\|\sigma\|_{DG}\|\omega\|_{DG}+\chi\Delta t\|\phi\|\|\omega\|+\gamma\Delta t\|\sigma\|\|\omega\|\\&\le C_1(\|\phi\|_{DG}+|R|+\|\sigma\|_{DG})(\|\theta\|_{DG}+\|\omega\|_{DG}+|Q|).\end{aligned}\tag{25}$$

In what follows, by taking $(\theta,\omega,Q)=(\phi,\sigma,R)$, using Young's inequality, we can prove $\mathcal{F}(\cdot,\cdot)$ is coercive.

$$\begin{aligned}&\mathcal{F}((\phi,\sigma,R),(\phi,\sigma,R))\\&=\|\phi\|^2+\lambda\Delta t\|\|\phi\|\|^2+\alpha\Delta t\|\phi\|^2+2\Delta tR^2+\|\sigma\|^2\\&\quad+\beta\Delta t\|\|\sigma\|\|^2-\chi\Delta t(\phi,\sigma)+\gamma\Delta t\|\sigma\|^2\\&\ge\|\phi\|^2+\lambda\Delta t\|\|\phi\|\|^2+\alpha\Delta t\|\phi\|^2+2\Delta tR^2+\beta\Delta t\|\|\sigma\|\|^2\\&\quad+\|\sigma\|^2-\frac{\chi}{2}\Delta t\|\sigma\|^2-\frac{\chi}{2}\Delta t\|\phi\|^2+\gamma\Delta t\|\sigma\|^2\\&\ge C_2(\|\phi\|^2+|R|^2+\|\phi\|_{DG}^2+\|\sigma\|^2+\|\sigma\|_{DG}^2)\\&\ge C_3(\|\phi\|_{DG}^2+|R|^2+\|\sigma\|_{DG}^2),\end{aligned}\tag{26}$$

where constants $C_1,C_2,C_3\ge0$ depend on $\Delta t,\lambda,\alpha,\beta,\chi,\gamma$ and $\chi\le2\alpha$ or 2γ.

Therefore, we can derive that the scheme (14)-(15) admits a unique solution using the Lax-Milgram theorem. □

3.3. Energy stability. The following is the unconditional energy stability of the proposed scheme (14)-(15).

Theorem 3.6. *The scheme (14)-(15) preserves an energy dissipation law unconditionally*

(27)

$$\begin{aligned}&E_{tot}^h(\phi_h^{n+1},\sigma_h^{n+1})+\frac{\lambda}{2}\|\|\phi_h^{n+1}-\phi_h^n\|\|^2+\frac{\alpha}{2}\|\phi_h^{n+1}-\phi_h^n\|^2+\frac{\beta}{2}\|\|\sigma_h^{n+1}-\sigma_h^n\|\|^2\\&+\frac{\gamma}{2}\|\sigma_h^{n+1}-\sigma_h^n\|^2+|R_h^{n+1}-R_h^n|^2+\frac{\|\phi_h^{n+1}-\phi_h^n\|^2}{\Delta t}+\frac{\|\sigma_h^{n+1}-\sigma_h^n\|^2}{\Delta t}=E_{tot}^h(\phi_h^n,\sigma_h^n).\end{aligned}$$

By a simple trentment, we can obtain the following discrete energy dissipation law

$$E_{tot}^h(\phi_h^{n+1},\sigma_h^{n+1})\le E_{tot}^h(\phi_h^n,\sigma_h^n),\tag{28}$$

where the modified total energy E_{tot}^h is defined as

$$\begin{aligned}E_{tot}^h(\phi_h^n,\sigma_h^n)=&\frac{\lambda}{2}\|\|\phi_h^n\|\|^2+\frac{\alpha}{2}\|\phi_h^n\|^2+\frac{\beta}{2}\|\|\sigma_h^n\|\|^2\\&+\frac{\gamma}{2}\|\sigma_h^n\|^2+|R_h^n|^2-(s,\sigma_h^n)-\chi(\sigma_h^n,\phi_h^n)-B.\end{aligned}\tag{29}$$

Proof. First of all, we introduce the following identity

$$a(a-b) = \frac{1}{2}(|a|^2 - |b|^2 + |a-b|^2). \tag{30}$$

Setting $\theta_h = (\phi_h^{n+1} - \phi_h^n)$ in (14a) and from (30) , we can have

$$\begin{aligned}&\frac{\|\phi_h^{n+1} - \phi_h^n\|^2}{\Delta t} - \chi(\sigma_h^n, \phi_h^{n+1} - \phi_h^n) + \frac{\lambda}{2}(|||\phi_h^{n+1}|||^2 - |||\phi_h^n|||^2 + |||\phi_h^{n+1} - \phi_h^n|||^2)\\ &+ \frac{\alpha}{2}(||\phi_h^{n+1}||^2 - ||\phi_h^n||^2 + ||\phi_h^{n+1} - \phi_h^n||^2) + \frac{R_h^{n+1}}{\sqrt{E_1(\phi_h^n)}}(f(\phi_h^n), \phi_h^{n+1} - \phi_h^n) = 0.\end{aligned} \tag{31}$$

Letting $\omega_h = (\sigma_h^{n+1} - \sigma_h^n)$ in (15) and from (30), we can obtain

$$\begin{aligned}&\frac{\|\sigma_h^{n+1} - \sigma_h^n\|^2}{\Delta t} + \frac{\gamma}{2}(\|\sigma_h^{n+1}\|^2 - \|\sigma_h^n\|^2 + \|\sigma_h^{n+1} - \sigma_h^n\|^2) - (s, \sigma_h^{n+1} - \sigma_h^n)\\ &- \chi(\phi_h^{n+1}, \sigma_h^{n+1} - \sigma_h^n) + \frac{\beta}{2}(|||\sigma_h^{n+1}|||^2 - |||\sigma_h^n|||^2 + |||\sigma_h^{n+1} - \sigma_h^n|||^2) = 0.\end{aligned} \tag{32}$$

Multiplying by $2R_h^{n+1}$ in (14b), and using (30) leads to

$$|R_h^{n+1}|^2 - |R_h^n|^2 + |R_h^{n+1} - R_h^n|^2 = \frac{R_h^{n+1}}{\sqrt{E_1(\phi_h^n)}}(f(\phi_h^n), \phi_h^{n+1} - \phi_h^n). \tag{33}$$

Adding the above equations (31)-(33), we can obtain

$$\begin{aligned}&\frac{\|\phi_h^{n+1} - \phi_h^n\|^2}{\Delta t} + \frac{\|\sigma_h^{n+1} - \sigma_h^n\|^2}{\Delta t} - (s, \sigma_h^{n+1} - \sigma_h^n)\\ &+ \frac{\lambda}{2}(|||\phi_h^{n+1}|||^2 - |||\phi_h^n|||^2 + |||\phi_h^{n+1} - \phi_h^n|||^2)\\ &+ \frac{\beta}{2}(|||\sigma_h^{n+1}|||^2 - |||\sigma_h^n|||^2 + |||\sigma_h^{n+1} - \sigma_h^n|||^2)\\ &+ \frac{\alpha}{2}(||\phi_h^{n+1}||^2 - ||\phi_h^n||^2 + ||\phi_h^{n+1} - \phi_h^n||^2)\\ &+ \frac{\gamma}{2}(\|\sigma_h^{n+1}\|^2 - \|\sigma_h^n\|^2 + \|\sigma_h^{n+1} - \sigma_h^n\|^2) + |R_h^{n+1}|^2 - |R_h^n|^2 + |R_h^{n+1} - R_h^n|^2\\ &+ \chi(\sigma_h^n, \phi_h^n) - \chi(\phi_h^{n+1}, \sigma_h^{n+1}) = 0.\end{aligned} \tag{34}$$

Substituting the above formula into (29), we can have

$$\begin{aligned}&\frac{\lambda}{2}|||\phi_h^{n+1}|||^2 + \frac{\alpha}{2}\|\phi_h^{n+1}\|^2 + \frac{\beta}{2}|||\sigma_h^{n+1}|||^2 + \frac{\gamma}{2}\|\sigma_h^{n+1}\|^2 + |R_h^{n+1}|^2 - (s, \sigma_h^{n+1})\\ &- \chi(\sigma_h^{n+1}, \phi_h^{n+1}) + \frac{\lambda}{2}|||\phi_h^{n+1} - \phi_h^n|||^2 + \frac{\alpha}{2}\|\phi_h^{n+1} - \phi_h^n\|^2 + \frac{\beta}{2}|||\sigma_h^{n+1} - \sigma_h^n|||^2\\ &+ \frac{\gamma}{2}\|\sigma_h^{n+1} - \sigma_h^n\|^2 + |R_h^{n+1} - R_h^n|^2 + \frac{\|\phi_h^{n+1} - \phi_h^n\|^2}{\Delta t} + \frac{\|\sigma_h^{n+1} - \sigma_h^n\|^2}{\Delta t}\\ &= \frac{\lambda}{2}|||\phi_h^n|||^2 + \frac{\alpha}{2}\|\phi_h^n\|^2 + \frac{\beta}{2}|||\sigma_h^n|||^2 + \frac{\gamma}{2}\|\sigma_h^n\|^2 + |R_h^n|^2 - (s, \sigma_h^n) - \chi(\sigma_h^n, \phi_h^n),\end{aligned} \tag{35}$$

it directly achieves (27). □

4. Numerical Analysis

Based on the fully discrete numerical scheme (14)-(15) established in the Section 3, we will analyze the optimal error estimates of ϕ and σ in terms of space and time discretization.

In what follows, we introduce the following concepts for all $n \geq 0$

$$
\begin{aligned}
&e_\phi^n = \phi(t_n) - \phi_h^n = \xi_\phi^n + \eta_\phi^n, \qquad \xi_\phi^n = \phi(t_n) - \mathcal{Q}_h\phi^n, \qquad \eta_\phi^n = \mathcal{Q}_h\phi^n - \phi_h^n,\\
&e_\sigma^n = \sigma(t_n) - \sigma_h^n = \xi_\sigma^n + \eta_\sigma^n, \qquad \xi_\sigma^n = \sigma(t_n) - \mathcal{F}_h\sigma^n, \qquad \eta_\sigma^n = \mathcal{F}_h\sigma^n - \sigma_h^n,\\
&e_R^n = R(t_n) - R_h^n.
\end{aligned}
$$

In particular, we assume the solutions to the system (9) satisfy

$$
\begin{cases}
\phi, \sigma \in L^\infty(0,T; H^{k+1}(\Omega) \cap L^\infty(\Omega)),\\
\phi_t, \sigma_t \in L^\infty(0,T; H^{k+1}(\Omega) \cap H^2(\Omega)),\\
\phi_{tt} \in L^\infty(0,T; H^2(\Omega)), \sigma_{tt} \in L^\infty(0,T; L^2(\Omega)).
\end{cases} \tag{36}
$$

By the lemma 2.2 and Theorem 3.6, there exists

$$
\|\phi(t)\| \leq K,\ \|\nabla\phi(t)\| \leq K,\ \|\phi_h^n\| \leq K,\ \|\phi_h^n\|_{DG} \leq K, \tag{37}
$$

where contant K depends on ϕ_0, T and Ω. From (36) and (37), we can have

$$
|f(\phi(t))| \leq K,\ |f'(\phi(t))| \leq K,\ |f(\phi_h^n)| \leq K,\ |f'(\phi_h^n)| \leq K. \tag{38}
$$

As shown below, the exact solution of system (9) comlpies with the truncation forms for any $0 \leq n \leq N-1$.

$$
\begin{aligned}
(\frac{\phi(t_{n+1}) - \phi(t_n)}{\Delta t}, \theta) = &-\lambda\mathcal{A}_1(\phi(t_{n+1}), \theta) - \frac{R(t_{n+1})}{\sqrt{E_1(\phi(t_n))}}(f(\phi(t_n)), \theta)\\
&+ \chi(\sigma(t_{n+1}), \theta) - \alpha(\phi(t_{n+1}), \theta) + (E_\phi^n, \theta),
\end{aligned} \tag{39a}
$$

$$
\begin{aligned}
(\frac{\sigma(t_{n+1}) - \sigma(t_n)}{\Delta t}, \omega) = &-\beta\mathcal{A}_2(\sigma(t_{n+1}), \omega) + \chi(\phi(t_{n+1}), \omega) + (s, \omega)\\
&- \gamma(\sigma(t_{n+1}), \omega) + (E_\sigma^n, \omega),
\end{aligned} \tag{39b}
$$

$$
R(t_{n+1}) - R(t_n) = \frac{1}{2\sqrt{E_1(\phi(t_n))}}(f(\phi(t_n)), \phi(t_{n+1}) - \phi(t_n)) + \Delta t E_R^n, \tag{39c}
$$

where

$$
\begin{aligned}
&E_\phi^n = R(t_{n+1})[\frac{f(\phi(t_n))}{\sqrt{E_1(\phi(t_n))}} - \frac{f(\phi(t_{n+1}))}{\sqrt{E_1(\phi(t_{n+1}))}}] + \frac{\phi(t_{n+1}) - \phi(t_n)}{\Delta t} - \phi_t(t_{n+1}),\\
&E_\sigma^n = \frac{\sigma(t_{n+1}) - \sigma(t_n)}{\Delta t} - \sigma_t(t_{n+1}),\\
&E_R^n = \frac{R(t_{n+1}) - R(t_n)}{\Delta t} - R_t(t_n) - \frac{1}{2\sqrt{E_1(\phi(t_n))}}(\frac{\phi(t_{n+1}) - \phi(t_n)}{\Delta t} - \phi_t(t_n), f(\phi(t_n))).
\end{aligned}
$$

Lemma 4.1. *Based on the regularity assumption (36), the truncation errors E_ϕ^n, E_σ^n and E_R^n comply that*

$$
\max_{1 \leq n \leq N}(\|E_\phi^n\| + \|E_\sigma^n\| + |E_R^n|) \lesssim \Delta t. \tag{40}
$$

Proof. Using Taylor formula, we can get

$$\begin{aligned}\|E_\phi^n\| =&|R(t_{n+1})|\|(\frac{f(\phi(t_{n+1}))}{\sqrt{E_1(\phi(t_{n+1}))}}-\frac{f(\phi(t_n))}{\sqrt{E_1(\phi(t_n))}})\|+|\delta_t\phi(t_{n+1})-\phi_t(t_{n+1})|\\ \le&\max_{0\le t\le T}|R(t)|(\frac{|E_1(\phi(t_{n+1}))-E_1(\phi(t_n))|\|f(\phi(t_n))\|}{(\sqrt{E_1(\phi(t_{n+1}))}+\sqrt{E_1(\phi(t_n))})\sqrt{E_1(\phi(t_{n+1}))E_1(\phi(t_n))}}\\ &+\frac{\|f(\phi(t_{n+1}))-f(\phi(t_n))\|}{\sqrt{E_1(\phi(t_{n+1}))}})+C\int_{t_n}^{t_{n+1}}|\phi_{tt}(s)|ds\\ \le&C(\max_{0\le t\le T}|R(t)|,\|\phi\|_{L^\infty(L^\infty)},\|\phi_t\|_{L^\infty(H^1)})\Delta t+C\int_{t_n}^{t_{n+1}}|\phi_{tt}(s)|ds\le C\Delta t,\end{aligned}$$

$$|E_\sigma^n|=|\delta_t\sigma(t_{n+1})-\sigma_t(t_{n+1})|\le C\int_{t_n}^{t_{n+1}}|\sigma_{tt}(s)|ds\le C\Delta t.$$

By (36) and (38), it can be easily checked that

$$\begin{aligned}R_{tt}=&-\frac{1}{4\sqrt{E_1(\phi)^3}}(\int f(\phi)\phi_t d\boldsymbol{x})^2+\frac{1}{2\sqrt{E_1(\phi)}}\int(f'(\phi)\phi_t^2+f(\phi)\phi_{tt})d\boldsymbol{x}\\ \le&C(\|f(\phi)\|^2\|\phi_t\|^2_{L^6(\Omega)}+\|f'(\phi)\|\|\phi_t\|^2_{L^6(\Omega)}+\|f(\phi)\|\|\phi_{tt}\|)\\ \le&C(\|\phi_t\|^2_{H^1(\Omega)}+\|\phi_{tt}\|),\end{aligned}$$

then we can get

$$\begin{aligned}|E_R^n|=&|\delta_tR(t_{n+1})-R_t(t_n)-\frac{1}{2\sqrt{E_1(\phi(t_n))}}\int_\Omega f(\phi(t_n))(\delta_t\phi(t_{n+1})-\phi_t(t_n))d\boldsymbol{x}|\\ \le&C(\int_{t_n}^{t_{n+1}}|R_{tt}(s)|ds+\int_{t_n}^{t_{n+1}}\int_\Omega|\phi_{tt}(s)|d\boldsymbol{x}ds)\le C\Delta t.\end{aligned}$$

Summing up the above estimates, it directly achieves (40). □

Theorem 4.2. *Suppose that the scheme (14)-(15) has unique solutions $\phi_h^{n+1},\sigma_h^{n+1},R_h^{n+1}$. Under the regularity assumption of (36), we have the following estimates for any $m=0,1,\cdots,N-1$.*

$$\begin{aligned}&\|e_\phi^{m+1}\|^2+\|e_\sigma^{m+1}\|^2+2|e_R^{m+1}|^2+\sum_{n=0}^m\|e_\phi^{n+1}-e_\phi^n\|^2\\ &+\sum_{n=0}^m\|e_\sigma^{n+1}-e_\sigma^n\|^2+2\sum_{n=0}^m|e_R^{n+1}-e_R^n|^2+\lambda\Delta t\sum_{n=0}^m\|e_\phi^{n+1}\|^2_{DG}\\ &+\beta\Delta t\sum_{n=0}^m\|e_\sigma^{n+1}\|^2_{DG}+\alpha\Delta t\sum_{n=0}^m\|e_\phi^{n+1}\|^2+\gamma\Delta t\sum_{n=0}^m\|e_\sigma^{n+1}\|^2\\ &\lesssim\Delta t^2+h^{2k}.\end{aligned}\tag{41}$$

Proof. Firstly, the difference between (14)-(15) and (39) gives the following error equations

$$\begin{aligned}(\frac{e_\phi^{n+1}-e_\phi^n}{\Delta t},\theta_h)=&-\lambda\mathcal{A}_1(e_\phi^{n+1},\theta_h)-\frac{R(t_{n+1})}{\sqrt{E_1(\phi(t_n))}}(f(\phi(t_n)),\theta_h)-\alpha(e_\phi^{n+1},\theta_h)\\ &+\chi(e_\sigma^n,\theta_h)+\frac{R_h^{n+1}}{\sqrt{E_1(\phi_h^n)}}(f(\phi_h^n),\theta_h)\\ &+\chi(\sigma(t_{n+1})-\sigma(t_n),\theta_h)+(E_\phi^n,\theta_h),\end{aligned}\tag{42}$$

$$
\begin{aligned}
(\frac{e_\sigma^{n+1}-e_\sigma^n}{\Delta t},\omega_h) =& -\beta\mathcal{A}_2(e_\sigma^{n+1},\omega_h)+\chi(e_\phi^{n+1},\omega_h)\\
&-\gamma(e_\sigma^{n+1},\omega_h)+(E_\sigma^n,\omega_h),
\end{aligned}
\tag{43}
$$

$$
\begin{aligned}
e_R^{n+1}-e_R^n =& \frac{1}{2\sqrt{E_1(\phi(t_n))}}(f(\phi(t_n)),\phi(t_{n+1})-\phi(t_n))\\
&-\frac{1}{2\sqrt{E_1(\phi_h^n)}}(f(\phi_h^n),\phi_h^{n+1}-\phi_h^n)+\Delta t E_R^n.
\end{aligned}
\tag{44}
$$

Using (11) and (12), we can obtain

$$
\begin{aligned}
&(\frac{\eta_\phi^{n+1}-\eta_\phi^n}{\Delta t},\theta_h)+\lambda\mathcal{A}_1(\eta_\phi^{n+1},\theta_h)-\chi(\eta_\sigma^n,\theta_h)+\alpha(\eta_\phi^{n+1},\theta_h)\\
&=-(\frac{\xi_\phi^{n+1}-\xi_\phi^n}{\Delta t},\theta_h)+\chi(\xi_\sigma^n,\theta_h)-\alpha(\xi_\phi^{n+1},\theta_h)-\frac{e_R^{n+1}}{\sqrt{E_1(\phi_h^n)}}(f(\phi_h^n),\theta_h)\\
&+R(t_{n+1})(\frac{f(\phi_h^n)}{\sqrt{E_1(\phi_h^n)}}-\frac{f(\phi(t_n))}{\sqrt{E_1(\phi(t_n))}},\theta_h)+\chi(\sigma(t_{n+1})-\sigma(t_n),\theta_h)+(E_\phi^n,\theta_h),
\end{aligned}
\tag{45}
$$

$$
\begin{aligned}
&(\frac{\eta_\sigma^{n+1}-\eta_\sigma^n}{\Delta t},\omega_h)+\beta\mathcal{A}_2(\eta_\sigma^{n+1},\omega_h)-\chi(\eta_\phi^{n+1},\omega_h)+\gamma(\eta_\sigma^{n+1},\omega_h)\\
&=-(\frac{\xi_\sigma^{n+1}-\xi_\sigma^n}{\Delta t},\omega_h)+\chi(\xi_\phi^{n+1},\omega_h)-\gamma(\xi_\sigma^{n+1},\omega_h)+(E_\sigma^n,\omega_h),
\end{aligned}
\tag{46}
$$

$$
\begin{aligned}
e_R^{n+1}-e_R^n =& \frac{1}{2}(\frac{f(\phi(t_n))}{\sqrt{E_1(\phi(t_n))}}-\frac{f(\phi_h^n)}{\sqrt{E_1(\phi_h^n)}},\phi(t_{n+1})-\phi(t_n))\\
&+\frac{1}{2}(\frac{f(\phi_h^n)}{\sqrt{E_1(\phi_h^n)}},\xi_\phi^{n+1}-\xi_\phi^n)+\frac{1}{2}(\frac{f(\phi_h^n)}{\sqrt{E_1(\phi_h^n)}},\eta_\phi^{n+1}-\eta_\phi^n)+\Delta t E_R^n.
\end{aligned}
\tag{47}
$$

Taking $\theta_h=\Delta t\eta_\phi^{n+1}$ in (45), we can derive

$$
\begin{aligned}
&(\eta_\phi^{n+1}-\eta_\phi^n,\eta_\phi^{n+1})+\lambda\Delta t\mathcal{A}_1(\eta_\phi^{n+1},\eta_\phi^{n+1})-\chi\Delta t(\eta_\sigma^n,\eta_\phi^{n+1})+\alpha\Delta t(\eta_\phi^{n+1},\eta_\phi^{n+1})\\
&=-(\xi_\phi^{n+1}-\xi_\phi^n,\eta_\phi^{n+1})+\chi\Delta t(\xi_\sigma^n,\eta_\phi^{n+1})-\alpha\Delta t(\xi_\phi^{n+1},\eta_\phi^{n+1})\\
&\quad-\frac{e_R^{n+1}}{\sqrt{E_1(\phi_h^n)}}\Delta t(f(\phi_h^n),\eta_\phi^{n+1})+R(t_{n+1})\Delta t(\frac{f(\phi_h^n)}{\sqrt{E_1(\phi_h^n)}}-\frac{f(\phi(t_n))}{\sqrt{E_1(\phi(t_n))}},\eta_\phi^{n+1})\\
&\quad+\chi\Delta t(\sigma(t_{n+1})-\sigma(t_n),\eta_\phi^{n+1})+\Delta t(E_\phi^n,\eta_\phi^{n+1}).
\end{aligned}
\tag{48}
$$

Setting $\omega_h=\Delta t\eta_\sigma^{n+1}$ from (46), we can obtain

$$
\begin{aligned}
&(\eta_\sigma^{n+1}-\eta_\sigma^n,\eta_\sigma^{n+1})+\beta\Delta t\mathcal{A}_2(\eta_\sigma^{n+1},\eta_\sigma^{n+1})-\chi\Delta t(\eta_\phi^{n+1},\eta_\sigma^{n+1})+\gamma\Delta t(\eta_\sigma^{n+1},\eta_\sigma^{n+1})=\\
&-(\xi_\sigma^{n+1}-\xi_\sigma^n,\eta_\sigma^{n+1})+\chi\Delta t(\xi_\phi^{n+1},\eta_\sigma^{n+1})-\gamma\Delta t(\xi_\sigma^{n+1},\eta_\sigma^{n+1})+\Delta t(E_\sigma^n,\eta_\sigma^{n+1}).
\end{aligned}
\tag{49}
$$

Multiplying (47) by $2e_R^{n+1}$ leads to

$$
\begin{aligned}
2e_R^{n+1}(e_R^{n+1}-e_R^n) =& e_R^{n+1}(\frac{f(\phi(t_n))}{\sqrt{E_1(\phi(t_n))}}-\frac{f(\phi_h^n)}{\sqrt{E_1(\phi_h^n)}},\phi(t_{n+1})-\phi(t_n))\\
&+e_R^{n+1}(\frac{f(\phi_h^n)}{\sqrt{E_1(\phi_h^n)}},\xi_\phi^{n+1}-\xi_\phi^n)+e_R^{n+1}(\frac{f(\phi_h^n)}{\sqrt{E_1(\phi_h^n)}},\eta_\phi^{n+1}-\eta_\phi^n)+2\Delta t E_R^n e_R^{n+1}.
\end{aligned}
\tag{50}
$$

Combining (48)-(50), using Lemma 3.1, then we can derive

$$
\begin{aligned}
(51)\quad & \frac{1}{2}(\|\eta_\phi^{n+1}\|^2 - \|\eta_\phi^n\|^2 + \|\eta_\phi^{n+1} - \eta_\phi^n\|^2) \\
& + \frac{1}{2}(\|\eta_\sigma^{n+1}\|^2 - \|\eta_\sigma^n\|^2 + \|\eta_\sigma^{n+1} - \eta_\sigma^n\|^2) + |e_R^{n+1}|^2 \\
& - |e_R^n|^2 + |e_R^{n+1} - e_R^n|^2 + \lambda\Delta t\|\eta_\phi^{n+1}\|_{DG}^2 \\
& + \beta\Delta t\|\eta_\sigma^{n+1}\|_{DG}^2 + \alpha\Delta t\|\eta_\phi^{n+1}\|^2 + \gamma\Delta t\|\eta_\sigma^{n+1}\|^2 \\
\lesssim & \Delta t(E_\phi^n, \eta_\phi^{n+1}) + \Delta t(E_\sigma^n, \eta_\sigma^{n+1}) + 2\Delta t E_R^n e_R^{n+1} \\
& + \chi\Delta t(\eta_\phi^{n+1}, \eta_\sigma^{n+1}) + \chi\Delta t(\eta_\phi^{n+1}, \eta_\sigma^n) \\
& - \alpha\Delta t(\xi_\phi^{n+1}, \eta_\phi^{n+1}) - \gamma\Delta t(\xi_\sigma^{n+1}, \eta_\sigma^{n+1}) + \chi\Delta t(\xi_\phi^{n+1}, \eta_\sigma^{n+1}) + \chi\Delta t(\eta_\phi^{n+1}, \xi_\sigma^n) \\
& - (\xi_\phi^{n+1} - \xi_\phi^n, \eta_\phi^{n+1}) - (\xi_\sigma^{n+1} - \xi_\sigma^n, \eta_\sigma^{n+1}) + \chi\Delta t(\sigma(t_{n+1}) - \sigma(t_n), \eta_\phi^{n+1}) \\
& - \frac{e_R^{n+1}}{\sqrt{E_1(\phi_h^n)}}\Delta t(f(\phi_h^n), \eta_\phi^{n+1}) + R(t_{n+1})\Delta t(\frac{f(\phi_h^n)}{\sqrt{E_1(\phi_h^n)}} - \frac{f(\phi(t_n))}{\sqrt{E_1(\phi(t_n))}}, \eta_\phi^{n+1}) \\
& + e_R^{n+1}(\frac{f(\phi(t_n))}{\sqrt{E_1(\phi(t_n))}} - \frac{f(\phi_h^n)}{\sqrt{E_1(\phi_h^n)}}, \phi(t_{n+1}) - \phi(t_n)) \\
& + e_R^{n+1}(\frac{f(\phi_h^n)}{\sqrt{E_1(\phi_h^n)}}, \eta_\phi^{n+1} - \eta_\phi^n) + e_R^{n+1}(\frac{f(\phi_h^n)}{\sqrt{E_1(\phi_h^n)}}, \xi_\phi^{n+1} - \xi_\phi^n) \\
= & I_1 + I_2 + ... + I_{16} + I_{17}.
\end{aligned}
$$

By use of the Cauchy-Schwarz inequality, Lemma 4.1 and Young's inequality, we can derive

$$(52)\qquad I_1 = \Delta t(E_\phi^n, \eta_\phi^{n+1}) \lesssim \Delta t^3 + \frac{\alpha}{20}\Delta t\|\eta_\phi^{n+1}\|^2.$$

$$(53)\qquad I_2 = \Delta t(E_\sigma^n, \eta_\sigma^{n+1}) \lesssim \Delta t^3 + \frac{\gamma}{8}\Delta t\|\eta_\sigma^{n+1}\|^2.$$

$$(54)\qquad I_3 = 2\Delta t E_R^n e_R^{n+1} \lesssim \Delta t^3 + \Delta t|e_R^{n+1}|^2.$$

$$(55)\qquad I_4 = \chi\Delta t(\eta_\phi^{n+1}, \eta_\sigma^{n+1}) \lesssim \frac{\gamma}{8}\Delta t\|\eta_\sigma^{n+1}\|^2 + \frac{\alpha}{20}\Delta t\|\eta_\phi^{n+1}\|^2.$$

$$(56)\qquad I_5 = \chi\Delta t(\eta_\phi^{n+1}, \eta_\sigma^n) \lesssim \Delta t\|\eta_\sigma^n\|^2 + \frac{\alpha}{20}\Delta t\|\eta_\phi^{n+1}\|^2.$$

From the Cauchy-Schwarz inequality, (13), lemma 3.4 and Young's inequality, we can have

$$(57)\qquad I_6 = -\alpha\Delta t(\xi_\phi^{n+1}, \eta_\phi^{n+1}) \lesssim \Delta t h^{2k+2} + \frac{\alpha}{20}\Delta t\|\eta_\phi^{n+1}\|^2.$$

$$(58)\qquad I_7 = -\gamma\Delta t(\xi_\sigma^{n+1}, \eta_\sigma^{n+1}) \lesssim \Delta t h^{2k+2} + \frac{\gamma}{8}\Delta t\|\eta_\sigma^{n+1}\|^2.$$

$$(59)\qquad I_8 = \chi\Delta t(\xi_\phi^{n+1}, \eta_\sigma^{n+1}) \lesssim \Delta t h^{2k+2} + \frac{\gamma}{8}\Delta t\|\eta_\sigma^{n+1}\|^2.$$

$$(60)\qquad I_9 = \chi\Delta t(\eta_\phi^{n+1}, \xi_\sigma^n) \lesssim \Delta t h^{2k+2} + \frac{\alpha}{20}\Delta t\|\eta_\phi^{n+1}\|^2.$$

(61)
$$I_{10} = -(\xi_\phi^{n+1} - \xi_\phi^n, \eta_\phi^{n+1}) = -\Delta t(\frac{\xi_\phi^{n+1} - \xi_\phi^n}{\Delta t}, \eta_\phi^{n+1}) \lesssim \int_{t_n}^{t_{n+1}} \|\frac{\partial \xi_\phi}{\partial t}\|^2 dt + \Delta t\|\eta_\phi^{n+1}\|^2$$
$$\lesssim h^{2k+2} \int_{t_n}^{t_{n+1}} \|\phi_t\|^2_{H^{k+1}(\mathcal{E}_h)} dt + \frac{\alpha}{20}\Delta t\|\eta_\phi^{n+1}\|^2.$$

(62)
$$I_{11} = -(\xi_\sigma^{n+1} - \xi_\sigma^n, \eta_\sigma^{n+1}) = -\Delta t(\frac{\xi_\sigma^{n+1} - \xi_\sigma^n}{\Delta t}, \eta_\sigma^{n+1})$$
$$\lesssim h^{2k+2} \int_{t_n}^{t_{n+1}} \|\sigma_t\|^2_{H^{k+1}(\mathcal{E}_h)} dt + \frac{\gamma}{8}\Delta t\|\eta_\sigma^{n+1}\|^2.$$

Applying the Young's inequality, (38) and Cauchy-Schwarz inequality, we can get

(63)
$$I_{12} = \chi\Delta t(\sigma(t_{n+1}) - \sigma(t_n), \eta_\phi^{n+1}) = \chi\Delta t^2(\frac{\sigma(t_{n+1}) - \sigma(t_n)}{\Delta t}, \eta_\phi^{n+1})$$
$$\lesssim \Delta t^3 + \frac{\alpha}{20}\Delta t\|\eta_\phi^{n+1}\|^2.$$

(64)
$$I_{13} = -e_R^{n+1}\Delta t(\frac{f(\phi_h^n)}{\sqrt{E_1(\phi_h^n)}}, \eta_\phi^{n+1}) \lesssim \Delta t|e_R^{n+1}|^2 + \frac{\alpha}{20}\Delta t\|\eta_\phi^{n+1}\|^2.$$

Then, we can get

$$\frac{f(\phi(t_n))}{\sqrt{E_1(\phi(t_n))}} - \frac{f(\phi_h^n)}{\sqrt{E_1(\phi_h^n)}}$$
$$= \frac{f(\phi(t_n)) - f(\phi_h^n)}{\sqrt{E_1(\phi(t_n))}} + \frac{(E_1(\phi_h^n) - E_1(\phi(t_n)))f(\phi_h^n)}{(\sqrt{(E_1(\phi(t_n))} + \sqrt{E_1(\phi_h^n)}))\sqrt{E_1(\phi(t_n))E_1(\phi_h^n)}},$$

and using the fact that $E_1(\phi) \geq C_0$ and (38), we can have

(65)
$$\|\frac{f(\phi(t_n))}{\sqrt{E_1(\phi(t_n))}} - \frac{f(\phi_h^n)}{\sqrt{E_1(\phi_h^n)}}\| \lesssim \|f(\phi(t_n)) - f(\phi_h^n)\| + (E_1(\phi_h^n) - E_1(\phi(t_n)))\|f(\phi_h^n)\|$$
$$\lesssim \|\phi(t_n) - \phi_h^n\| = \|e_\phi^n\|.$$

From the Cauchy-Schwarz inequality, $|R(t)| \leq C$, (65) and Young's inequality, we can get

(66)
$$I_{14} = -R(t_{n+1})\Delta t(\frac{f(\phi(t_n))}{\sqrt{E_1(\phi(t_n))}} - \frac{f(\phi_h^n)}{\sqrt{E_1(\phi_h^n)}}, \eta_\phi^{n+1})$$
$$\lesssim \Delta t|R(t_{n+1})|(e_\phi^n, \eta_\phi^{n+1}) \lesssim \Delta t h^{2k+2} + \Delta t\|\eta_\phi^n\|^2 + \frac{\alpha}{20}\Delta t\|\eta_\phi^{n+1}\|^2.$$

(67)
$$I_{15} = e_R^{n+1}(\frac{f(\phi(t_n))}{\sqrt{E_1(\phi(t_n))}} - \frac{f(\phi_h^n)}{\sqrt{E_1(\phi_h^n)}}, \phi(t_{n+1}) - \phi(t_n))$$
$$\lesssim \Delta t|e_R^{n+1}|\|\frac{f(\phi(t_n))}{\sqrt{E_1(\phi(t_n))}} - \frac{f(\phi_h^n)}{\sqrt{E_1(\phi_h^n)}}\|\|\frac{\phi(t_{n+1}) - \phi(t_n)}{\Delta t}\|$$
$$\lesssim \Delta t|e_R^{n+1}|^2 + \Delta t h^{2k+2} + \Delta t\|\eta_\phi^n\|^2.$$

Setting $\theta_h = \Delta t\frac{f(\phi_h^n)}{\sqrt{E_1(\phi_h^n)}}$ in (45), by applying the Cauchy-Schwarz inequality, (13), (65) and Young's inequality, we can arrive that

(68)
$$\begin{aligned}(\eta_\phi^{n+1}-\eta_\phi^n,\frac{f(\phi_h^n)}{\sqrt{E_1(\phi_h^n)}}) =& -(\xi_\phi^{n+1}-\xi_\phi^n,\frac{f(\phi_h^n)}{\sqrt{E_1(\phi_h^n)}}) - \lambda\Delta t\mathcal{A}_1(\eta_\phi^{n+1},\frac{f(\phi_h^n)}{\sqrt{E_1(\phi_h^n)}})\\ &+\chi\Delta t(e_\sigma^n,\frac{f(\phi_h^n)}{\sqrt{E_1(\phi_h^n)}}) - \alpha\Delta t(e_\phi^{n+1},\frac{f(\phi_h^n)}{\sqrt{E_1(\phi_h^n)}})\\ &-\Delta t\frac{e_R^{n+1}}{\sqrt{E_1(\phi_h^n)}}(f(\phi_h^n),\frac{f(\phi_h^n)}{\sqrt{E_1(\phi_h^n)}}) + \chi\Delta t(\sigma(t_{n+1})-\sigma(t_n),\frac{f(\phi_h^n)}{\sqrt{E_1(\phi_h^n)}})\\ &+R(t_{n+1})\Delta t(\frac{f(\phi_h^n)}{\sqrt{E_1(\phi_h^n)}}-\frac{f(\phi(t_n))}{\sqrt{E_1(\phi(t_n))}},\frac{f(\phi_h^n)}{\sqrt{E_1(\phi_h^n)}}) + \Delta t(E_\phi^n,\frac{f(\phi_h^n)}{\sqrt{E_1(\phi_h^n)}}),\end{aligned}$$

thus the term I_{16} can be bounded as

(69)
$$\begin{aligned}I_{16} =& e_R^{n+1}(\frac{f(\phi_h^n)}{\sqrt{E_1(\phi_h^n)}},\eta_\phi^{n+1}-\eta_\phi^n)\\ =& -e_R^{n+1}(\xi_\phi^{n+1}-\xi_\phi^n,\frac{f(\phi_h^n)}{\sqrt{E_1(\phi_h^n)}}) - \lambda\Delta t e_R^{n+1}\mathcal{A}_1(\eta_\phi^{n+1},\frac{f(\phi_h^n)}{\sqrt{E_1(\phi_h^n)}})\\ &+\chi\Delta t e_R^{n+1}(e_\sigma^n,\frac{f(\phi_h^n)}{\sqrt{E_1(\phi_h^n)}}) - \alpha\Delta t e_R^{n+1}(e_\phi^{n+1},\frac{f(\phi_h^n)}{\sqrt{E_1(\phi_h^n)}})\\ &-\Delta t\frac{e_R^{n+1}}{\sqrt{E_1(\phi_h^n)}}(f(\phi_h^n),\frac{f(\phi_h^n)}{\sqrt{E_1(\phi_h^n)}}) + \chi\Delta t e_R^{n+1}(\sigma(t_{n+1})-\sigma(t_n),\frac{f(\phi_h^n)}{\sqrt{E_1(\phi_h^n)}})\\ &+R(t_{n+1})\Delta t e_R^{n+1}(\frac{f(\phi_h^n)}{\sqrt{E_1(\phi_h^n)}}-\frac{f(\phi(t_n))}{\sqrt{E_1(\phi(t_n))}},\frac{f(\phi_h^n)}{\sqrt{E_1(\phi_h^n)}})\\ &+\Delta t e_R^{n+1}(E_\phi^n,\frac{f(\phi_h^n)}{\sqrt{E_1(\phi_h^n)}})\\ \lesssim& \Delta t\|\frac{\xi_\phi^{n+1}-\xi_\phi^n}{\Delta t}\|^2 + \Delta t|e_R^{n+1}|^2 + \Delta t\|\eta_\phi^{n+1}\|_{DG}^2\\ &+\Delta t\|e_\sigma^n\|^2 + \Delta t\|e_\phi^{n+1}\|^2 + \Delta t^3 + \Delta t\|e_\phi^n\|^2 + \Delta t\|E_\phi^n\|^2\\ \lesssim& (\Delta t^3+\Delta t h^{2k+2}) + \Delta t|e_R^{n+1}|^2 + \frac{\lambda}{4}\Delta t\|\eta_\phi^{n+1}\|_{DG}^2\\ &+\Delta t\|\eta_\sigma^n\|^2 + \frac{\alpha}{20}\Delta t\|\eta_\phi^{n+1}\|^2 + \Delta t\|\eta_\phi^n\|^2.\end{aligned}$$

From the Cauchy-Schwarz inequality, (13), (38) and Young's inequality, we can derive

(70)
$$\begin{aligned}I_{17} =& -e_R^{n+1}(\frac{f(\phi_h^n)}{\sqrt{E_1(\phi_h^n)}},\xi_\phi^{n+1}-\xi_\phi^n)\\ =& \Delta t e_R^{n+1}(\frac{f(\phi_h^n)}{\sqrt{E_1(\phi_h^n)}},\frac{\xi_\phi^{n+1}-\xi_\phi^n}{\Delta t})\\ \lesssim& \Delta t|e_R^{n+1}|^2 + h^{2k+2}\int_{t_n}^{t_{n+1}}\|\phi_t\|_{H^{k+1}(\mathcal{E}_h)}^2 dt.\end{aligned}$$

Combining with the above estimates, one obtains

$$
\begin{aligned}
&\frac{1}{2}(\|\eta_\phi^{n+1}\|^2-\|\eta_\phi^n\|^2+\|\eta_\phi^{n+1}-\eta_\phi^n\|^2)\\
&+\frac{1}{2}(\|\eta_\sigma^{n+1}\|^2-\|\eta_\sigma^n\|^2+\|\eta_\sigma^{n+1}-\eta_\sigma^n\|^2)+|e_R^{n+1}|^2\\
&-|e_R^n|^2+|e_R^{n+1}-e_R^n|^2+\frac{\lambda}{2}\Delta t\|\eta_\phi^{n+1}\|_{DG}^2\\
&+\frac{\beta}{2}\Delta t\|\eta_\sigma^{n+1}\|_{DG}^2+\frac{\alpha}{2}\Delta t\|\eta_\phi^{n+1}\|^2+\frac{\gamma}{2}\Delta t\|\eta_\sigma^{n+1}\|^2\\
&\lesssim \Delta t^3+\Delta t h^{2k+2}+\Delta t\|\eta_\phi^n\|^2+\Delta t\|\eta_\phi^{n+1}\|^2\\
&+\Delta t\|\eta_\sigma^n\|^2+\Delta t\|\eta_\sigma^{n+1}\|^2+\Delta t|e_R^{n+1}|^2.
\end{aligned}
\tag{71}
$$

Summing (71) over $n=0$ to $m\le N-1$, we can get

$$
\begin{aligned}
&\|\eta_\phi^{m+1}\|^2+\|\eta_\sigma^{m+1}\|^2+2|e_R^{m+1}|^2+\sum_{n=0}^{m}\|\eta_\phi^{n+1}-\eta_\phi^n\|^2\\
&+\sum_{n=0}^{m}\|\eta_\sigma^{n+1}-\eta_\sigma^n\|^2+2\sum_{n=0}^{m}|e_R^{n+1}-e_R^n|^2\\
&+\lambda\Delta t\sum_{n=0}^{m}\|\eta_\phi^{n+1}\|_{DG}^2+\beta\Delta t\sum_{n=0}^{m}\|\eta_\sigma^{n+1}\|_{DG}^2\\
&+\alpha\Delta t\sum_{n=0}^{m}\|\eta_\phi^{n+1}\|^2+\gamma\Delta t\sum_{n=0}^{m}\|\eta_\sigma^{n+1}\|^2\\
&\lesssim \Delta t\sum_{n=0}^{m}(\Delta t^2+h^{2k+2})\\
&+C_1\Delta t\sum_{n=0}^{m}(\|\eta_\phi^n\|^2+\|\eta_\phi^{n+1}\|^2+\|\eta_\sigma^n\|^2+\|\eta_\sigma^{n+1}\|^2+|e_R^{n+1}|^2).
\end{aligned}
\tag{72}
$$

When $0<\Delta t\le\Delta t_0:=\frac{1}{2C_1}<\frac{1}{C_1}$, since $1\le\frac{1}{1-C_1\Delta t}\le 2$ and from (72), we can get

$$
\begin{aligned}
&\|\eta_\phi^{m+1}\|^2+\|\eta_\sigma^{m+1}\|^2+2|e_R^{m+1}|^2+\sum_{n=0}^{m}\|\eta_\phi^{n+1}-\eta_\phi^n\|^2\\
&+\sum_{n=0}^{m}\|\eta_\sigma^{n+1}-\eta_\sigma^n\|^2+2\sum_{n=0}^{m}|e_R^{n+1}-e_R^n|^2\\
&+\lambda\Delta t\sum_{n=0}^{m}\|\eta_\phi^{n+1}\|_{DG}^2+\beta\Delta t\sum_{n=0}^{m}\|\eta_\sigma^{n+1}\|_{DG}^2\\
&+\alpha\Delta t\sum_{n=0}^{m}\|\eta_\phi^{n+1}\|^2+\gamma\Delta t\sum_{n=0}^{m}\|\eta_\sigma^{n+1}\|^2\\
&\lesssim \frac{\Delta t}{1-C_1\Delta t}\sum_{n=0}^{m}(\Delta t^2+h^{2k+2})\\
&\quad+\frac{C_1\Delta t}{1-C_1\Delta t}\sum_{n=0}^{m}(\|\eta_\phi^n\|^2+\|\eta_\phi^{n+1}\|^2+\|\eta_\sigma^n\|^2+\|\eta_\sigma^{n+1}\|^2+|e_R^{n+1}|^2).
\end{aligned}
\tag{73}
$$

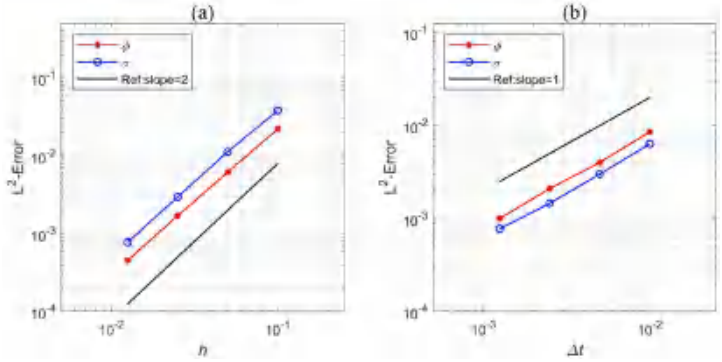

FIGURE 5.1. L^2 numerical error and convergence order for the approximation at time $t = 0.6$. (a): convergence order in spatial direction. (b): convergence order in temporal direction.

Applying the discrete Gronwall's inequality, we can have

$$
\begin{aligned}
&\|\eta_\phi^{m+1}\|^2 + \|\eta_\sigma^{m+1}\|^2 + 2|e_R^{m+1}|^2 + \sum_{n=0}^{m} \|\eta_\phi^{n+1} - \eta_\phi^n\|^2 \\
&+ \sum_{n=0}^{m} \|\eta_\sigma^{n+1} - \eta_\sigma^n\|^2 + 2\sum_{n=0}^{m} |e_R^{n+1} - e_R^n|^2 \\
&+ \lambda\Delta t \sum_{n=0}^{m} \|\eta_\phi^{n+1}\|_{DG}^2 + \beta\Delta t \sum_{n=0}^{m} \|\eta_\sigma^{n+1}\|_{DG}^2 \\
&+ \alpha\Delta t \sum_{n=0}^{m} \|\eta_\phi^{n+1}\|^2 + \gamma\Delta t \sum_{n=0}^{m} \|\eta_\sigma^{n+1}\|^2 \\
&\lesssim \Delta t^2 + h^{2k+2}.
\end{aligned} \tag{74}
$$

Using the triangle inequality, the proof is finished. □

5. Numerical examples

This section presents several numerical experiments to solve the tumor growth model by implementing the fully discrete scheme (14)-(15). Further, we use the $P_2 - P_2$ element for ϕ and σ, and we also use the scheme to simulate the variations of phase field function and nutrient function in tumor growth.

5.1. Accuracy and stability tests. The first numerical examples focuses on the convergence and energy stability of the proposed scheme. We consider the computational domain in the square $\Omega = [0, 2]^2$ $(unit : 10^3\mu m)$ and the total computational time is set as $T = 0.6$ $(unit : year)$. The initial conditions are chosen as

$$
\phi_0 = \begin{cases} 1, & 0.94 < x < 1.06 \text{ and } 0.80 < y < 1.20, \\ 0, & \text{otherwise}, \end{cases}
$$

$$
\sigma_0 = \begin{cases} \sin(2\pi x), & 0.94 < x < 1.06, \\ 0, & \text{otherwise}. \end{cases}
$$

The model parameters in this case are set as $\lambda = 160000\ \mu m^2/year$, $\varepsilon = 0.01\ year$, $\chi = 600\ L/(g \cdot year)$, $\alpha = 600\ 1/year$, $\beta = 5000000\ \mu m^2/year$, $s = 2.7\ g/(L \cdot day)$

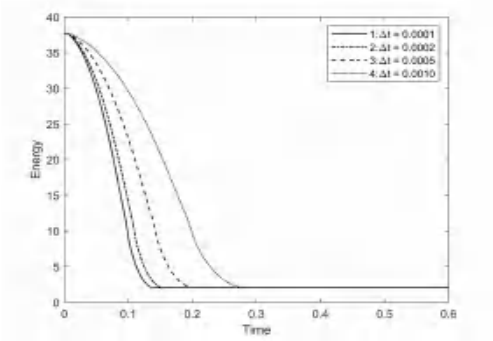

FIGURE 5.2. Time evolution of the total energy functional E_{tot}^h for $\Delta t = 0.0001$, 0.0002, 0.0005 and 0.0010.

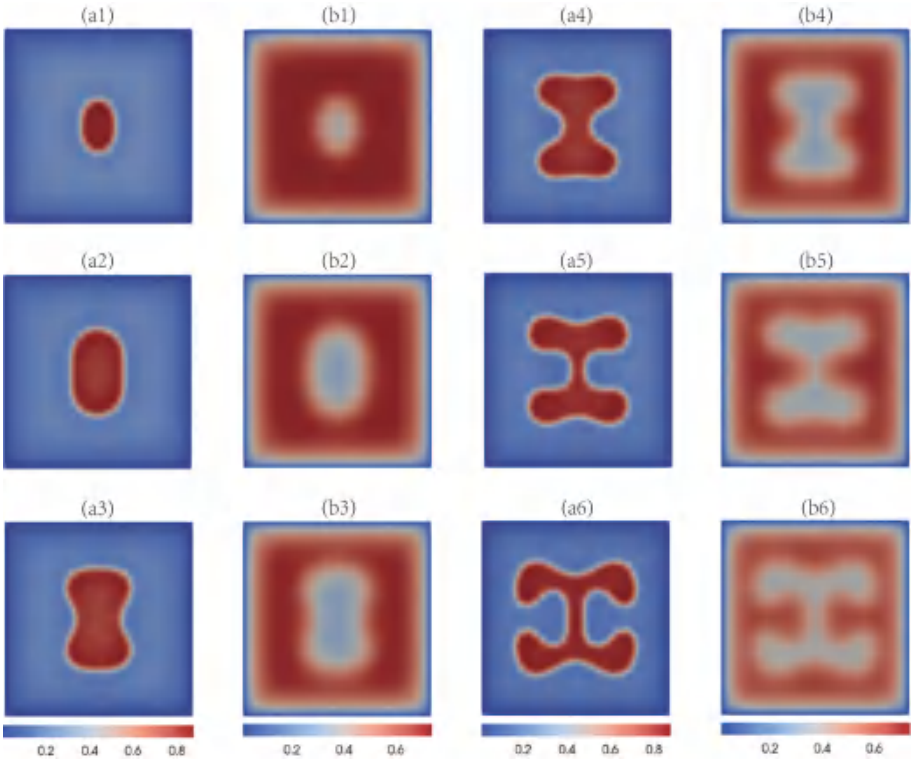

FIGURE 5.3. The evolution of the phase field function ϕ (the subfigures (a1)-(a6)) and nutrient function σ (the subfigures (b1)-(b6)) at $s = 2.60\ g/(L \cdot day)$ in the two dimensional case and different times for: (1) $t = 0.1$; (2) $t = 0.2$; (3) $t = 0.3$; (4) $t = 0.4$; (5) $t = 0.5$; (6) $t = 0.6$.

and $\gamma = 1000\ 1/year$. It is hard to get the exact solution of (2), and we compute the reference solution by taking time step size $\Delta t = 0.0001$ and mesh size $h = 1/120$.

To test the convergence behavior of spatial error, we choose the decreasing spatial step sizes $h = 1/10$, $1/20$, $1/40$ and $1/80$, and fix the time step size $\Delta t = 0.001$ to show the L^2 errors for the phase field function ϕ and nutrient function σ in

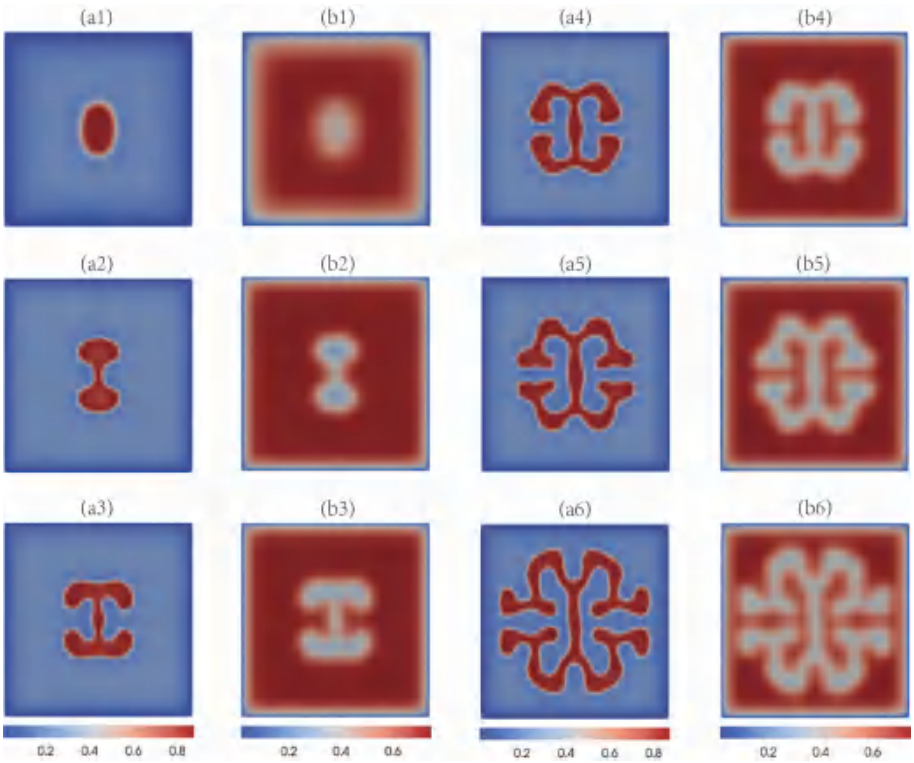

FIGURE 5.4. The evolution of the phase field function ϕ (the subfigures (a1)-(a6)) and nutrient function σ (the subfigures (b1)-(b6)) at $s = 2.70\ g/(L \cdot day)$ in the two dimensional case and different times for: (1) $t = 0.1$; (2) $t = 0.2$; (3) $t = 0.3$; (4) $t = 0.4$; (5) $t = 0.5$; (6) $t = 0.6$.

Fig. 5.1(a). It can be seen that the obtained spatial convergence rate is $\mathcal{O}(h^2)$, which is consistent with our theoretical prediction. In addition, to verify the convergence rates of temporal errors for the considered scheme, we perform the L^2 errors for the phase field function ϕ and nutrient function σ at $t = 0.6$ in Fig. 5.1(b), by fixing the spacial size $h = 1/80$ and choosing the temporal step sizes with $\Delta t = 0.00125$, 0.0025, 0.005 and 0.01. It is apparent that the order of convergence is $\mathcal{O}(\Delta t)$ for all variables, which is consistent with the theoretical analysis.

In Fig. 5.2, we compute the discrete energy E_{tot}^h dissipation of the considered scheme with different time steps $\Delta t = 0.0001$, 0.0002, 0.0005 and 0.0010. It can be seen that the total energy of the system is dissipated regardless of the time step taken, and the rate of dissipation slows down as the time step increases, but the energy still tends to dissipate.

5.2. Growth of tumors in 2D. This subsection primarily aims to validate the capability of the numerical scheme (14)-(15) in illustrating the tumor growth. In the following numerical example, we consider the tumor growth of choosing different values of the nutrient supply in 2D. We take the computational domain $\Omega = [0, 2]^2$ $(unit : 10^3 \mu m)$ with $T = 2.0$ $(unit : year)$. We set temporal step size $\Delta t = 0.0001$ and spacial size $h = 0.01$. The nutrient supply parameter s is set as $2.60\ g/(L \cdot day)$, $2.70\ g/(L \cdot day)$ and $2.80\ g/(L \cdot day)$, other parameters are fixed

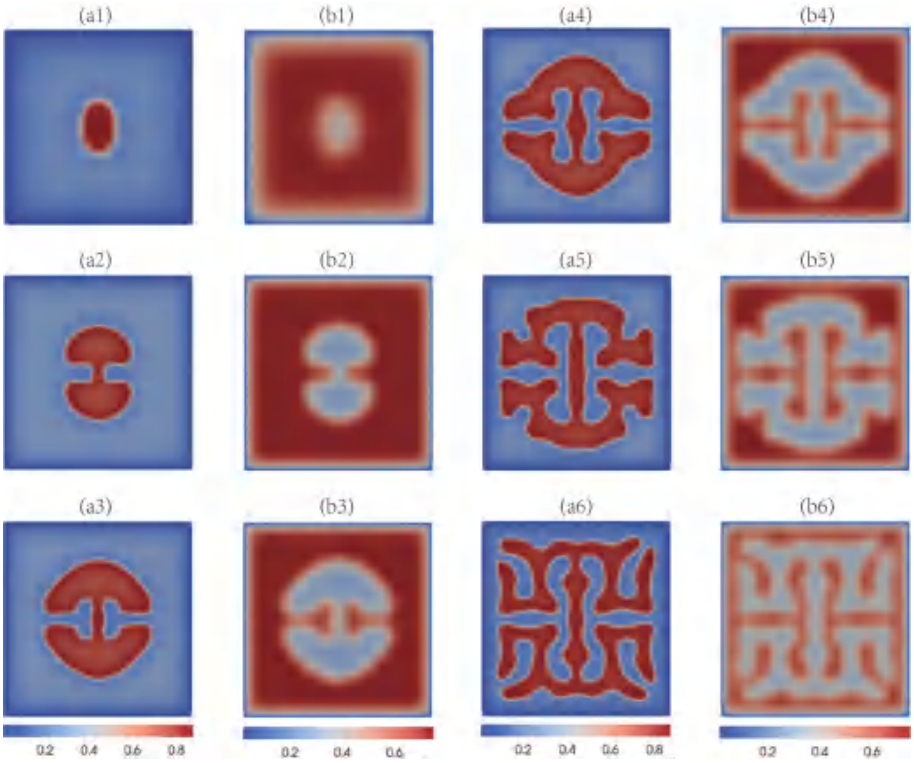

FIGURE 5.5. The evolution of the phase field function ϕ (the subfigures (a1)-(a6)) and nutrient function σ (the subfigures (b1)-(b6)) at $s = 2.80\ g/(L \cdot day)$ in the two dimensional case and different times for: (1) $t = 0.1$; (2) $t = 0.2$; (3) $t = 0.3$; (4) $t = 0.4$; (5) $t = 0.5$; (6) $t = 0.6$.

as previous subsection. $\phi = 0$ and $\sigma = 0$ are imposed on all boundaries, and the initial conditions are the same as in the previous subsection.

In Fig. 5.3, Fig. 5.4 and Fig. 5.5, we give the simulation results with s is $2.60\ g/(L \cdot day)$, $2.70\ g/(L \cdot day)$ and $2.80\ g/(L \cdot day)$, respectively. We show the evolution of the phase field function ϕ and nutrient function σ at time $t = 0.1, 0.2, 0.3, 0.4, 0.5$ and 0.6. The two dimensional simulation results are similar to previous studies, and can be seen in [34] and [35].

5.3. Growth of tumors in 3D. In this example, we study the tumor growth in 3D based on the proposed DG scheme. We choose the computational domain $\Omega = [0, 2]^3$ $(unit : 10^3 \mu m)$ with $T = 2.0$ $(unit : year)$. We set temporal step size $\Delta t = 0.0006$ and spacial size $h = 0.04$. The model parameters and boundary conditions are the same as in the previous subsection and the initial conditions are set as follows

$$\phi_0 = \begin{cases} 1, & 0.94 < x < 1.06,\ 0.80 < y < 1.20\ and\ 0.80 < z < 1.20, \\ 0, & otherwise, \end{cases}$$

$$\sigma_0 = \begin{cases} \sin(2\pi x), & 0.94 < x < 1.06, \\ 0, & otherwise. \end{cases}$$

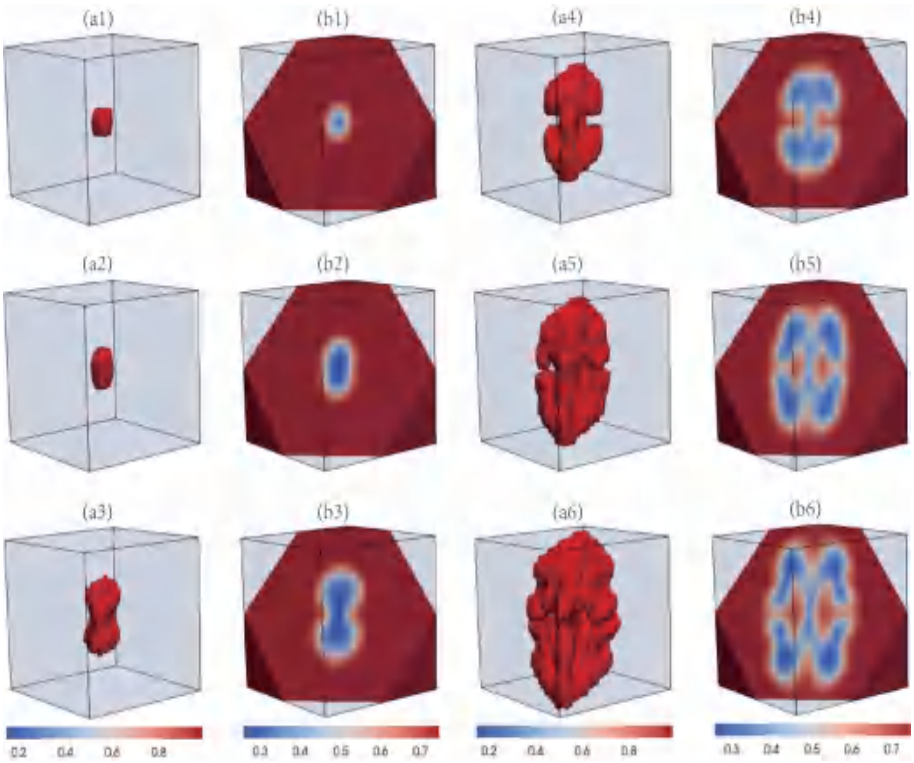

FIGURE 5.6. The evolution of the phase field function ϕ (the subfigures (a1)-(a6)) and nutrient function σ (the subfigures (b1)-(b6)) at $s = 2.60\ g/(L \cdot day)$ in the three dimensional case and different times for: (1) $t = 0.1$; (2) $t = 0.2$; (3) $t = 0.3$; (4) $t = 0.4$; (5) $t = 0.5$; (6) $t = 0.6$.

In Fig. 5.6 and Fig. 5.7, we also give the simulation results with s is $2.60\ g/(L{\cdot}day)$ and $2.70\ g/(L{\cdot}day)$, respectively. We show the evolution of the phase field function ϕ and nutrient function σ at time $t = 0.1, 0.2, 0.3, 0.4, 0.5$ and 0.6. It can be observed that when the $s = 2.60\ g/(L \cdot day)$, the fingered morphology grows thinner and branches less. Through to increase the nutrition value s to $2.70\ g/(L \cdot day)$, the tumor of the fingered morphology produce wider branches. It can also be observed that the tumor grows slowly when s is small. However, the growth rate of the tumor will accelerate, when increasing s to 2.70. At the same time, the results in this paper and those reported in [33] indicate that the tumor initially grows in a spherical shape. If the tumor continues to develop in this morphology, it will consume more nutrients and the concentration of nutrient will decrease. With a constant supply of nutrients, the simulation results show that the supply of nutrients and the growth of the tumor reached a steady state when $t = 0.55$, the pattern of tumor does not change, and finally appeared as a fingered morphology.

6. Conclusion and outlook

In this paper, we firstly derive a tumor growth model based on free energy. For this model, the scalar auxiliary variable (SAV) is used to handle the nonlinear term. Combining the backward Euler (BDF1) method and the discontinuous

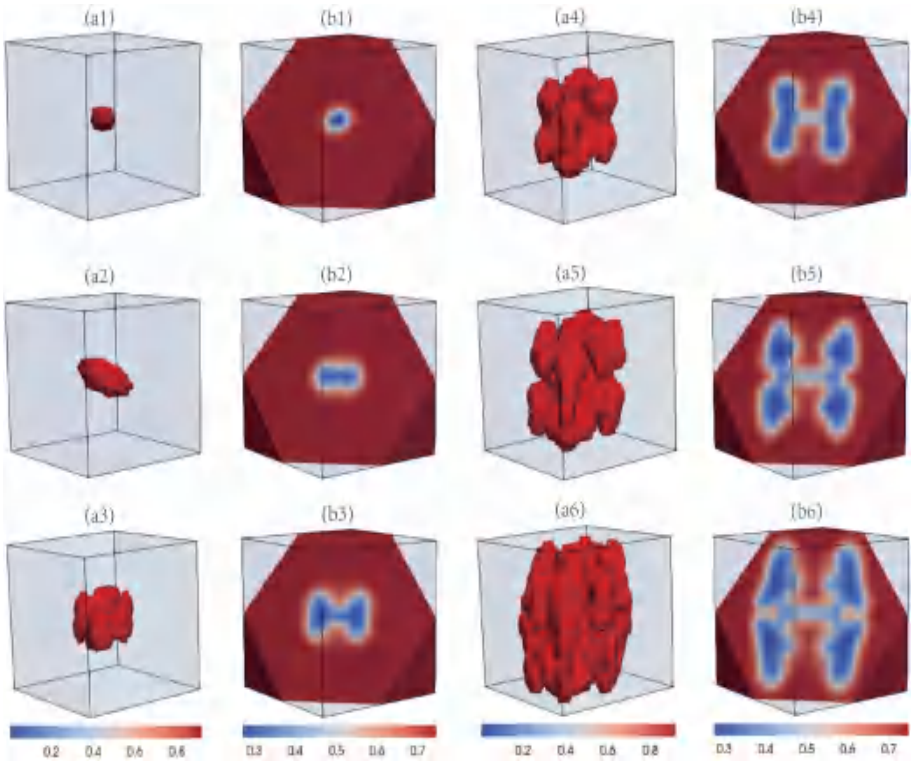

FIGURE 5.7. The evolution of the phase field function ϕ (the subfigures (a1)-(a6)) and nutrient function σ (the subfigures (b1)-(b6)) at $s = 2.70\ g/(L \cdot day)$ in the three dimensional case and different times for: (1) $t = 0.1$; (2) $t = 0.2$; (3) $t = 0.3$; (4) $t = 0.4$; (5) $t = 0.5$; (6) $t = 0.6$.

Galerkin (DG) method to discretize the model, we propose a linear, fully decoupled and unconditionally energy stable numerical scheme. The rigorous and detailed proof processes of solvability and stability are given, and we prove optimal error estimates of the related variables through strict theoretical analysis. Through some numerical experiments, the validity of the model and numerical scheme are demonstrated numerically. In addition, the tumor growth process is simulated by numerical scheme. However, our study is an isotropic equation, while the growth of real tumor is anisotropic, that is a great challenge will be considered in future work.

Acknowledgements

The authors are grateful to the reviewers for the constructive comments and valuable suggestions which have improved the paper. Bo Wang is supported by the National Natural Science Foundation of China (No. 42430702) and the Natural Science Foundation of Henan Province (No. 232300420109). Guang-an Zou is supported by the Key Scientific Research Projects of Colleges and Universities in Henan Province, China (23A110006).

References

[1] J. Ferlay, M. Colombet, I. Soerjomataram, D. M. Parkin, M. Piñeros, A. Znaor, F. Bray, Cancer statistics for the year 2020, an overview, Int J Cancer, 149(4), 778-799, 2021.

[2] J. Ferlay, M. Colombet, I. Soerjomataram, C. Mathers, D. M. Parkin, M. Piñeros, A. Znaor, F. Bray, Estimating the global cancer incidence and mortality in 2018: Globocan sources and methods, Int J Cancer, 144(8), 1941-1953, 2019.

[3] F. Bray, J. Ferlay, I. Soerjomataram, R. L. Siegel, L. A. Torre, A. Jemal, Global cancer statistics 2018: Globocan estimates of incidence and mortality worldwide for 36 cancers in 185 countries, CA Cancer J Clin, 68(6), 394-424, 2018.

[4] J. Ferlay, M. Colombet, I. Soerjomataram, T. Dyba, G. Randi, M. Bettio, A. Gavin, O. Visser, F. Bray, Cancer incidence and mortality patterns in Europe: Estimates for 40 countries and 25 major cancers in 2018, Eur J Cancer, 103(10), 356-387, 2018.

[5] T. S. Deisboeck, L. Zhang, J. Yoon, J. Costa, In silico cancer modeling: Is it ready for prime time, Nat Clin Pract Oncol, 6(1), 34-42, 2009.

[6] H. M. Byrne, Dissecting cancer through mathematics: From the cell to the animal model, Nat Rev Cancer, 10(3), 221-230, 2010.

[7] C. R. Thoma, M. Zimmermann, I. Agarkova, J. M. Kelm, W. Krek, 3D cell culture systems modeling tumor growth determinants in cancer target discovery, Adv Drug Deliv Rev, 69(70), 29-41, 2014.

[8] Y. Imamura, T. Mukohara, Y. Shimono, N. Chayahara, M. Toyoda, N. Kiyota, S. Takao, S. Kono, T. Nakatsura, H. Minami, Comparison of 2D and 3D culture models as drug testing platforms in breast cancer, Oncol Rep, 33(4), 1837-1843, 2015.

[9] D. Antoni, H. Burckel, E, Josset, G. Noel, Three dimensional cell culture: A breakthrough in vivo, Int J Mol Sci, 16(3), 5517-5527, 2015.

[10] C. F. Ruivo, B. Adem, M. Silva, S. A. Melo, The Biology of Cancer Exosomes: Insights and New Perspectives, Cancer Res, 77(23), 1C9, 2017.

[11] J. R. Aunan, W. C. Cho, S. Kjetil, The biology of aging and cancer: A brief overview of shared and divergent molecular hallmarks, Aging Dis, 8(5), 628-642, 2017.

[12] E. D. Yorke, Z. Fuks, L. Norton, Modeling the development of metastases from primary and locally recurrent tumors: Comparison with a clinical data base for prostatic cancer, Cancer Res, 53(13), 2987-2993, 1993.

[13] T. L. Jackson, A mathematical model of prostate tumor growth and androgen independent relapse, Discrete Cont Dyn-B, 4(1), 187-201, 2004.

[14] A. M. Ideta, G. Tanaka, T. Takeuchi, K. Aihara, A mathematical model of intermittent androgen suppression for prostate cancer, J Nonlinear Sci, 18(6), 593, 2008.

[15] T. Shimada, K. Aihara, A nonlinear model with competition between prostate tumor cells and its application to intermittent androgen suppression therapy of prostate cancer, Math Biosci, 214(1-2), 134-139, 2008.

[16] A. Friedman, F. Reitich, Analysis of a mathematical model for the growth of tumors, J Math Biol, 38(3), 262-284, 1999.

[17] M. A. J. Chaplain, S. R. McDougall, A. R. A. Anderson, Mathematical modeling of tumor induced angiogenesis, J Math Biol, 49(2), 111-187, 2004.

[18] D. Grecu, A. S. Carstea, A. T. Grecu, A. Visinescu, Mathematical modelling of tumor growth, Roma Rep Phys, 59(2), 447-455, 2007.

[19] Q. Guo, Y. Tao, K. Aihara, Mathematical modeling of prostate tumor growth under intermittent androgen suppression with partial differential equations, Int J Bifurcat Chaos, 18(12), 3789-3797, 2008.

[20] Y. Tao, Q. Guo, K. Aihara, A mathematical model of prostate tumor growth under hormone therapy with mutation inhibitor, J Nonlinear Sci, 20(2), 219-240, 2010.

[21] A. Friedman, H. V. Jain, A partial differential equation model of metastasized prostatic cancer, Math Biosci Eng, 10(3), 591-608, 2013.

[22] J. Yang, T. J. Zhao, C. Q. Yuan, A nonlinear competitive model of the prostate tumor growth under intermittent androgen suppression, J Theor Biol, 404(5), 66-72, 2016.

[23] S. M. Wise, J. S. Lowengrub, H. B. Frieboes, V. Cristini, Three dimensional multispecies nonlinear tumor growth I model and numerical method, Opt Commun, 253(3), 524-543, 2008.

[24] A. Agosti, P. F. Antonietti, P. Ciarletta, M. Grasselli, M. Verani, A Cahn-Hilliard type equation with application to tumor growth dynamics, Math Methods Appl Sci, 10(2), 45-74, 2013.

[25] P. Colli, G. Gilardi, D. Hilhorst, On a Cahn-Hilliard type phase field system related to tumor growth, Discrete Cont Dyn A, 35(6), 2423-2442, 2014.
[26] P. Colli, G. Gilardi, E. Rocca, J. Sprekels, Vanishing viscosities and error estimate for a Cahn-Hilliard type phase field system related to tumor growth, Nonlinear Anal Real, 7(57), 40-59, 2015.
[27] H. G. Lee, Kim, Y. Kim, J. Kim, Mathematical model and its fast numerical method for the tumor growth, Math Biosci Eng, 12(6), 1173-1187, 2015.
[28] G. Lorenzo, M. A. Scott, K. Tew, Hierarchically refined and coarsened splines for moving interface problems, with particular application to phase field models of prostate tumor growth, Comput Method Appl M, 319(1), 515-548, 2017.
[29] X. Feng, Y. Li, Analysis of interior penalty discontinuous Galerkin methods for the Allen-Cahn equation and the mean curvature flow, IMA J Numer Anal, 35(4), 1622-1651, 2014.
[30] J. Shen, J. Xu, Unconditionally bound preserving and energy dissipative schemes for a class of Keller-Segel equations, SIAM J Numer Anal, 58(3), 1674-1695, 2020.
[31] H. Li, Z. Song, J. Hu, Numerical analysis of a second order IPDGFE method for the Allen-Cahn equation and the curvature driven geometric flow, Comput Math Appl, 86(6), 49-62, 2021.
[32] V. Mohammadi, M. Dehghan, Simulation of the phase field Cahn-Hilliard and tumor growth models via a numerical scheme: Element free Galerkin method, Comput Method Appl M, 11(19), 25-70, 2019.
[33] G. Lorenzo, M. A. Scott, K. Tew, T. J. Hughes, Y. J. Zhang, L. Liu, G. Vilanova, H. Gomez, Tissue scale, personalized modeling and simulation of prostate cancer growth, Proc Natl Acad Sci, 113(48), 7663-7671, 2016.
[34] V. Mohammadi, M. Dehghan, S. D. Marchi, Numerical simulation of a prostate tumor growth model by the RBF-FD scheme and a semi implicit time discretization, J Comput Appl Math, 20(1), 388-431, 2021.
[35] V. Mohammadi, M. Dehghana, A. Khodadadianc, N. Noii, T. Wick, An asymptotic analysis and numerical simulation of a prostate tumor growth model via the generalized moving least squares approximation combined with semi implicit time integration, Appl Math Model, 104(30), 826-849, 2022.
[36] E. Y. Medina, E. M. Toledo, I. Igreja, B. M. Rocha, A stabilized hybrid discontinuous Galerkin method for the Cahn-Hilliard equation, J Comput Appl M, 25(4), 406-431, 2022.
[37] Z. Xu, X. Yang, H. Zhang, Error analysis of a decoupled, linear stabilization scheme for the Cahn-Hilliard model of two phase incompressible flows, J Sci Comput, 83(3), 57-84, 2020.
[38] G. Zou, B. Wang, X. Yang, A fully decoupled discontinuous Galerkin approximation of the Cahn-Hilliard-Brinkman-Ohta-Kawasaki tumor growth model, ESAIM: M2AN, 56(6), 2141-2180, 2022.
[39] X. Yang, Linear, first and second order, unconditionally energy stable numerical schemes for the phase field model of homopolymer blends, J Comput Phys, 32(7), 294-316, 2016.
[40] X. Yang, I. Li, Linear and unconditionally energy stable schemes for the binary fluid surfactant phase field model, Comput Method Appl M, 2(11), 1005-1029, 2017.
[41] J. Shen, J. Xu, Convergence and error analysis for the Scalar Auxiliary Variable (SAV) schemes to gradient flows, SIAM J Numer Anal, 56(5), 2895-2912, 2018.
[42] Q. Cheng, J. Shen, Multiple Scalar Auxiliary Variable (MSAV) approach and its application to the phase field vesicle membrane model, SIAM J Sci Comput, 40(6), 3982-4006, 2018.
[43] X. Li, J. Shen, H. Rui, Energy stability and convergence of SAV block centered finite difference method for gradient flows, Math Comput, 31(9), 88-109, 2018.
[44] Z. Zheng, G. Zou, B. Wang, W. Zhao, A fully decoupled discontinuous Galerkin method for the nematic liquid crystal flows with SAV approach, J Comput Appl Math, 42(9), 115-142, 2023.
[45] B. Rivière, M. Wheeler, V. Girault, Improved energy estimates for interior penalty, constrained and discontinuous Galerkin methods for elliptic problems, Comput Geosci, 3(4), 337-360, 1999.
[46] A. Dn, F. Brezzi, B. Cockburn, Unified analysis of discontinuous Galerkin methods for elliptic problems, SIAM J Numer Anal, 39(5), 1749-1779, 2002.
[47] X. Feng, O. A. Karakashian, Fully discrete dynamic mesh discontinuous Galerkin methods for the Cahn-Hilliard equation of phase transition, Math Comput, 76(259), 1093-1117, 2007.
[48] B. Rivière, Discontinuous Galerkin methods for solving elliptic and parabolic equations: Theory and implementation, SIAM ebook, 2008.

[49] D. Kay, V. Styles, E. Sli, Discontinuous Galerkin finite element approximation of the Cahn-Hilliard equation with convection, SIAM J Numer Anal, 47(4), 2660-2685, 2009.
[50] A. C. Aristotelous, O. Karakashian, S. M. Wise, A mixed discontinuous Galerkin, convex splitting scheme for a modified Cahn-Hilliard equation and an efficient nonlinear multigrid solver, Discrete Cont Dyn-B, 18(9), 2211-2238, 2013.
[51] X. Feng, T. Lewis, Nonstandard local discontinuous Galerkin methods for fully nonlinear second order elliptic and parabolic equations in high dimensions, J Sci Comput, 77(1), 1534-1565, 2018.
[52] C. Liu, B. Rivière, Numerical analysis of a discontinuous Galerkin method for Cahn-Hilliard-Navier-Stokes equations, Mathematics Basel, 27(25), 1807-1838, 2018.
[53] G. Zou, B. Wang, X. Yang, Efficient interior penalty discontinuous Galerkin projection method with unconditional energy stability and second order temporal accuracy for the incompressible magneto hydrodynamic system, J Comput Phys, 25(6), 495-504, 2023.
[54] G. Zou, Z. Li, X. Yang, Fully discrete discontinuous Galerkin numerical scheme with second order temporal accuracy for the hydrodynamically coupled lipid vesicle model, J Sci Comput, 95(1), 23-70, 2023.

School of Mathematics and Statistics, Henan University, Kaifeng 475004, P. R. China
E-mail: guo-grape@163.com

School of Mathematics and Statistics, Henan University, Kaifeng 475004, P. R. China, Henan Key Laboratory of Earth System Observation and Modeling, Henan University, Kaifeng 475004, P. R. China, The Academy for Advanced Interdisplinary Studies, Henan University, Zhengzhou 450046, P. R. China
E-mail: wb2008@henu.edu.cn

School of Mathematics and Statistics, Henan University, Kaifeng 475004, P. R. China, Henan Key Laboratory of Earth System Observation and Modeling, Henan University, Kaifeng 475004, P. R. China, Center for Applied Mathematics of Henan Province, Henan University, Zhengzhou, 450046, China
E-mail: zouguangan@henu.edu.cn